ELSEVIER

Coordination Chemistry Reviews 233–234 (2002) 157–176

COORDINATION CHEMISTRY REVIEWS

www.elsevier.com/locate/ccr

Group 10 metal indenyl complexes

Davit Zargarian *

Département de Chimie, Université de Montréal, Montréal, Québec, Canada H3C 3J7

Received 21 December 2001; accepted 27 May 2002

Contents

Abstract

This review summarises the synthesis, characterisation, and reactivities of Group 10 metal indenyl complexes reported up to the end of 2001. We begin with a brief summary of the various arguments which have been put forth over the years to explain the observed differences between the reactivities of transition metal indenyl and cyclopentadienyl complexes. The main discussion is then focused on the various metal–indenyl bonding modes and preliminary reactivity trends observed in the complexes $(indenyl)_2Ni^{II}$, $\{(indenyl)Pd^{I}L\}_2$, $(indenyl)M^{II}LX$, and $[(indenyl)M^{II}LL']^+$ (M = Ni, Pd, Pt; L and X are neutral and anionic ligands,[1] respectively).

Keywords: Indenyl; Indenyl effect; Hapticity; Catalysis

1. Introduction

Transition metal complexes bearing Ind ligands (Ind = indenyl anion or radical and its substituted derivatives) have often been compared to their Cp analogues (Cp = cyclopentadienyl anion or radical and

* Tel.: +1-514-343-2247; fax: +1-514-343-7586
E-mail address: zargarian.davit@umontreal.ca (D. Zargarian).

[1] Throughout this review, L and X are used to denote neutral ligands such as PR_3, CO, olefin, etc. and anionic fragments such as Cl^-, Me^-, NR_2^-, etc., respectively. In the terminology of the covalent bonding model, X and L are donors of one and two electrons, respectively.

0010-8545/02/$ - see front matter
PII: S0010-8545(02)00201-1

its substituted derivatives) in terms of the kinetics of the ligand substitution reactions in these complexes. In general, the complexes $IndML_n$ undergo exchange of the ligands L at faster rates in comparison to $CpML_n$. This so-called "indenyl effect" has been invoked in numerous reports to account for the greater reactivity of Ind complexes both in catalysis [1] and in stoichiometric reactions (e.g. ligand substitution [2], insertion [3], etc.). Although various manifestations of the indenyl effect have been observed in many different compounds, most of the studies that have examined this phenomenon in detail have been focussed on the complexes of Groups 6, 8, and 9 metals.[2] A growing number of recent reports have also examined the different types of metal–Ind interactions and new reactivities observed for the Ind complexes of Group 10 metals (Ni [4–9]; Pd [10–13]; Pt [14]). Although the study of the latter complexes is still at a very early phase of its development, the rich pattern of bonding and reactivity already emerging from the structural and reactivity studies reported to date bodes well for the future development of this field of study.

This review aims to summarise the existing structural and reactivity data on the known Ind complexes of Group 10 metals. The material presented here covers reports published up to the end of 2001 and is organised according to the type of complex being discussed. Thus, the first ever reported Group 10 metal indenyl complex, $Ni(Ind)_2$, and its substituted homologues, (1-{(−)-3-menthyl}-4,7-Me_2–Ind)$_2$Ni and (2-Ph–Ind)$_2$Ni, are presented first. The neutral and cationic species IndM(L)(X) and $[IndM(L)(L')]^+$ are discussed next, including the complexes $\{(\mu\text{-Ind})Pd(L)\}_2$ that represent the only examples of Group 10 metal–Ind complexes in which the metal is not in the +2 oxidation state.

As background for the main discussion, it is important to appreciate the main arguments which have been put forth over the years to explain the differences in the reactivities of Ind and Cp complexes and to assess M–Ind interactions in various compounds. Thus, Section 2.1 gives an overview of the classical notion that the presence of the benzo ring facilitates the flexible hapticity of Ind ligands which, in turn, helps stabilise the transition states (or intermediates) of various reactions. This section also outlines the recent proposals pertaining to the importance of the ground state effects for the relative reactivities of Ind complexes (Sections 2.2 and 2.3). Then, Section 2.4 describes the methods that are used commonly to evaluate the Ind hapticity. Finally, Section 3 presents the available data on the structures and reactivities of Group 10 metal Ind complexes.

2. Background

2.1. The indenyl effect

The greater reactivity of Ind complexes in comparison to their Cp counterparts has been demonstrated most convincingly in a number of ligand exchange reactions. The earliest studies on the comparative kinetics of analogous Cp/Ind complexes involved the ligand substitution reactions of (Cp/Ind)$Mo(CO)_3X$. Hart–Davis and Mawby found, for example, that the reaction of (Cp/Ind)$Mo(CO)_3Me$ with PR_3 to give (Cp/Ind)$Mo(PR_3)(CO)_2(COMe)$ proceeds one or two orders of magnitude faster with the Ind analogue [15]. Kinetic studies showed that these reactions have negative $\Delta S^{\ddagger}$ values and their rates depended on $[PR_3]$, i.e. they follow an associative mechanism. Since the Cp and Ind starting complexes have virtually identical ν(CO) values (2023, 1944, and 1910 cm^{-1} for the Ind complex vs. 2023, 1942, and 1910 cm^{-1} for the Cp complex), these authors argued that the observed rate difference cannot be explained by ground state effects (i.e. weaker Mo–CO bonds). They proposed, instead, that the S_N2 reaction is facilitated by the displacement of the Ind with respect to Mo to give an intermediate (or activated complex) with an η^3-Ind; this would liberate a vacant orbital on the metal, thus facilitating the coordination of the incoming nucleophile. This idea was influenced by a similar rationale proposed earlier by Basolo and Schuster-Woldan [16] to account for the associative mechanism of the ligand substitution reaction involving $CpRh(CO)_2$; in this proposal, however, the authors invoked an attack by the incoming ligand on the Rh^+ centre in the zwitterionic intermediate (η^2,η^2-Cp)$Rh(CO)_2$.

Mawby's group also reported other interesting demonstrations of the superior reactivities of Ind complexes. For instance, they showed that the complexes $IndMo(CO)_3X$ (X = Cl, Br, I) undergo CO substitution by PR_3 at rates which are three to four orders of magnitude faster than the corresponding reactions with the Cp complexes [17]. Interestingly, the reactions of the Cp complexes were shown to follow a simple dissociative mechanism, whereas the Ind analogues followed a mechanism consisting of both dissociative and associative components. Shortly thereafter, Jones and Mawby showed that the complex $IndFe(CO)_2I$ undergoes CO substitution by an S_N1 (dissociative) mechanism and that the rate of this reaction is 600 times faster than the corresponding reactions with both the Cp and the tetrahydroindenyl analogues [18]. These results show unequivocally that it is the presence of a benzo ring in

[2] Many reports have also been carried out on the electronically unsaturated Ind complexes of early transition metals, and especially on the 16 electron Ind analogues of Group 4 metallocenes, but in these complexes the differences in the reactivities of the Cp and Ind complexes are mostly due to steric and symmetry factors and are not influenced by hapticity issues.

Ind which bestows faster ligand substitution rates to its complexes. In the case of associative substitutions, the faster rates found for Ind complexes were explained in terms of the $\eta^5 \rightarrow \eta^3$ slippage of Ind (vide supra). On the other hand, Mawby et al. speculated that the faster rates of dissociative substitutions with Ind complexes were due to the stabilisation of the electronically and coordinatively unsaturated intermediates as a result of the interaction of the benzo ring of Ind with the metal centre.

Consistent with Mawby's results, Huggins et al. have reported [19] that CO exchange is orders of magnitude faster in the complex $IndW(CO)_3Cl$ than in the analogous Cp complex; moreover, this reaction was found to proceed by a mixed associative–dissociative mechanism similar to that observed in the Mo complexes studied by Mawby, but at a much faster rate. Interestingly, the overall displacement of CO in this W complex was *accelerated* when the reaction was carried out under an atmosphere of CO! This observation was proposed as evidence for the involvement of an intermediate of the type $(\eta^3\text{-Ind})WL(CO)_3Cl$, which would form much more readily when L = CO; capture of this intermediate by the incoming nucleophile would thus result in an overall exchange of CO. A similar reasoning can be invoked to justify the greater rates of reactions in "apparently dissociative" ligand substitutions wherein solvent coordination can play a significant role, as shown in Scheme 1.

A number of kinetic studies involving complexes of Groups 7 and 9 metals have also been reported [20]. For

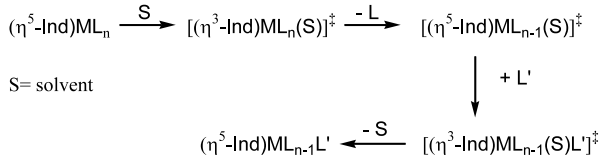

Scheme 1.

example, Basolo has shown that the CO exchange is relatively rapid in $IndMn(CO)_3$ whereas the Cp analogue is essentially inert [20a]. Moreover, Green et al. have shown [20b,20c] that $IndRh(C_2H_4)_2$ undergoes rapid exchange of both ethylene ligands by other olefins, dienes, alkynes, and isonitriles. In this system, an excess of isonitrile leads to the formation of either $(\eta^1\text{-Ind})Rh(CNR)_4$ or $[Rh(CNR)_4]^+[\eta^0\text{-Ind}]^-$, whereas a large excess of terminal alkynes leads to catalytic alkyne cyclotrimerisation. It is noteworthy that the corresponding Cp complex is inert toward this type of substitution. Finally, the significant discrepancy in the reactivities of some $Cp/IndRhL_n$ complexes is apparent from the remarkable rate difference of $K_{Ind}/K_{Cp} = 10^8$ measured by Basolo's group for the following reaction [20d]:

$$(\text{Ind or Cp})Rh(CO)_2 + PPh_3 \rightarrow (\text{Ind or Cp})Rh(CO)(PPh_3) + CO \quad (1)$$

The above results indicate that Ind ligands promote both dissociative and associative pathways, but their effects are much greater (ca. 10^5 times more) on the latter mechanism. The more facile dissociative reactions of $IndML_n$ complexes might arise from a better stabilisation of the ligand-dissociated species $IndML_{n-1}$ by the greater electron donation from Ind versus Cp [21]. On the other hand, the much more facile associative ligand substitution reactions of Ind complexes is often attributed to the well-documented propensity of Ind ligands to adopt lower than η^5 hapticities in order to accommodate additional electrons on the metal. According to this rationale, the association of an incoming ligand to the electronically saturated metal centre can be stabilised by the "slippage" of Ind to a lower mode of coordination; this has the effect of reducing the electron donation from Ind to the metal centre, thereby avoiding (or minimising) the build-up of excessive electron density on the metal. The destabilisation entailed by this reduction in Ind hapticity is counterbalanced by the re-aromatisation of the benzo moiety of the Ind ligand. Since this stabilisation mechanism is not available to Cp systems, this type of slippage is less favoured for Cp complexes and, consequently, associative ligand substitution reactions are generally slower in these complexes.

This phenomenon, which has been dubbed the "indenyl effect" by Basolo, is an example of the general notion that a so-called "ring slippage" should occur more easily with more highly conjugated ligands. Not surprisingly, the effect of rate acceleration via $\eta^5 \leftrightarrow \eta^3$ "ring slippage" is most noticeable for associative ligand substitutions in 18 electron complexes wherein the absence of reaction pathways involving ring-slipped species would lead to high energy, 20 electron intermediates (or activated complexes). Indeed, in cases where slippage is not involved, the rates of associative reactions are expected to be slower for the Ind complexes because of the more basic character and greater steric demands of Ind compared to Cp. The interplay between the steric and electronic properties of Ind substituents and their effects on the ground state structures and ligand substitution reactivities of the complexes $(R_n\text{–Ind})Rh(CO)_2$ have been examined by Marder, Basolo et al. [22]. As a new twist to the notion of "slippage", these authors propose that species arising from η^5-Ind to η^3-*exo*-Ind to η^5-Ind slippage mechanism might also be involved in the overall substitution pathway.

2.2. Ground state effects

In a clear departure from the arguments relating the increased reactivities of Ind complexes to transition state

effects, Kubas et al. have proposed that in some cases the higher kinetic reactivities of $IndML_n$ complexes might arise from their lower thermodynamic stabilities [23]. Thus, these authors have reported that the complex $IndW(CO)_3H$ is solvated readily to $L_3W(CO)_3$ (L = EtCN or THF; ΔH ca. −15 to −20 kcal mol^{-1}) whereas the corresponding Cp complex is stable under the same conditions. They estimate that the Ind analogue is thermodynamically less stable than its Cp counterpart by ca. 10–15 kcal mol^{-1}, and propose that it is this relative ground state instability of the Ind complex, rather than the stability of the transition states, which is responsible for the higher reactivity of the Ind complex. It should be noted, however, that the validity of this reasoning for the ligand substitution reactions in which the Ind remains coordinated to the metal has not been demonstrated yet.

2.3. Inverse indenyl effect

To complete this discussion, it is worth noting that while most studies have found Ind complexes to be more reactive than the corresponding Cp analogues, the opposite trend is also observed in some cases. For example, Sweigart et al. have demonstrated [24] that the dissociative substitution of CO in the 19 electron species $IndFe(CO)_3$, which are generated by electrochemical or chemical reduction of the 18 electron precursors $[IndFe(CO)_3]^+$, proceeds more slowly than the corresponding reaction in the analogous Cp species (Scheme 2).

This so-called "inverse indenyl effect" has been explained in terms not involving hapticity changes, as follows. According to these authors, the cause of this phenomenon is the presence of a low-lying π* orbital in the indenyl anion that is primarily localised in the benzo portion of this ligand. The interaction of this orbital of Ind with a LUMO of the $Fe(CO)_3^{2+}$ fragment gives the LUMO for $[IndFe(CO)_3]^+$ that is highly localised on the Ind and proportionately less localised on the Fe–CO bonds. Since the 19th electron can be placed in a LUMO which has a diminished Fe–CO character in the Ind complex compared to the Cp complex, it follows that the one-electron reduction of the Ind derivative causes less destabilisation of the Fe–CO bond (i.e. slower CO dissociation) than in the Cp analogue.

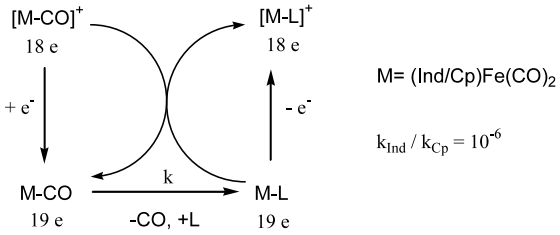

Scheme 2.

To sum up, the studies noted above demonstrate some of the significant differences between the reactivities of Ind/Cp complexes and outline the commonly accepted rationalisations for this phenomenon, meanwhile warning us to be mindful of a number of important factors such as the electronic configuration of the complexes (18 vs. 19 electrons) and different possible causes of reactivity differences (transition vs. ground state effects). In this context, studying the structures and reactivities of Group 10 metal–Ind complexes is interesting, given their potential to adopt a relatively wide range of electronic configurations (16–20 electrons) and the important implications this can have for their reactivities.

2.4. Measuring indenyl hapticity

Given the influence of M–Ind bonding modes on the reactivities of Ind complexes, a discussion of indenyl hapticity in terms of a number of structural parameters is an integral part of most reports on these complexes, including this review. To a first degree of simplification, the main features of Ind hapticity can be gleaned from a comparison of the bond distances from the metal centre to the C(1/3) carbon atoms of the allylic moiety versus the C(3a/7a) carbon atoms at the ring junction.[3] The difference between these distances can be used to determine the extent of the "slippage" of the Ind ligand away from an idealised pentahapto coordination.

A simple and generally employed method for quantifying "slippage" is based on the parameter ΔM–C; other useful parameters include the so-called hinge and fold angles (HA and FA). The definitions of ΔM–C, HA, and FA along with their values for a series of representative Ind complexes displaying a wide range of hapticities are given in Table 1; these data should

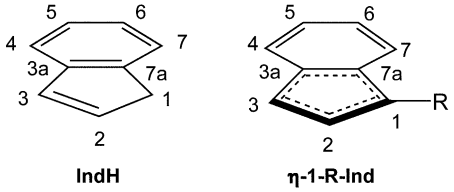

Chart 1.

[3] Comparison and cross referencing of the bonding modes among different complexes necessitates a uniform numbering scheme for denoting the various positions in Ind ligands. Unfortunately, different authors have tended to use different schemes in their reports. In order to facilitate the comparisons of M–Ind bonding modes among the known Group 10 metal Ind complexes, the numbering scheme shown in Chart 1 will be used throughout the present discussion; where necessary, the data from the primary sources have been adjusted to make them consistent with this scheme.

Table 1
Structural parameters for $M(Ind)_n L_m$

Compound	ΔM–C (Å) [a]	HA (°) [b]	FA (°) [c]	Ref.
$(\eta^5\text{-Ind})_2Fe$	0.043 [d]	2.2 [d]	0.8 [d]	[27b]
$\{(\eta^5\text{-Me}_7\text{Ind})RhCl(\mu\text{-Cl})\}_2$	0.087(5)	4.6		[46]
$(\eta\text{-Ind})Ir(Me)(Ph)(PMe_3)$	0.106(3)	–	5.7	[47]
$(\eta\text{-Ind})IrH_2(P^iPr_3)$	0.114	–	–	[48]
$(\eta\text{-Ind})_2Co$	0.124(4) [d]	7.6 [d]	6.0 [d]	[27b]
$(\eta\text{-Me}_7\text{Ind})RhCl_2(PMe_2Ph)$	0.154(3)	7.2	8.8	[46]
$(\eta\text{-Ind})Rh(\eta^2\text{-}C_2H_4)_2$	0.160(8)	–		[49]
$(\eta\text{-Ind})Rh(CO)_2$	0.20(1)	9.2	10.9	[50]
$(\eta\text{-Ind})Rh(PMe_3)_2$	0.201(4)	8.4	7.9	[51]
$(\eta\text{-Ind})(\eta\text{-Ind})V(CO)_2$	0.120(3) and 0.493(3)	–	12 [e]	[32]
$[(\eta^3\text{-Ind})Fe(CO)_3]^-$	0.689(7)	–	22	[29]
$(\eta^5\text{-Ind})(\eta^3\text{-Ind})W(CO)_2$	0.07(2) and 0.72(2)	–	26 [e]	[33]
$(\eta^3\text{-Ind})Ir(PMe_3)_3$	0.79(1)	–	28	[28]

[a] $\Delta M\text{–}C = 0.5\{(M\text{–}C(3a)+M\text{–}C(7a)\} - 0.5\{M\text{–}C(1)+M\text{–}C(3)\}$.
[b] HA is the angle formed between the planes formed by the atoms C(1), C(2), C(3) and C(1), C(3), C(3a), C(7a).
[c] FA is the angle formed between the planes formed by the atoms C(1), C(2), C(3) and C(3a), C(4), C(5), C(6), C(7), and C(7a).
[d] Average value over all the different Ind ligands present in the unit cell.
[e] This value is for the more slipped Ind ligand only.

provide a point of comparison for the main discussion outlined in Section 3. In general, the larger the ΔM–C, HA, and FA values for a given complex, the more extensive the "slippage" away from a pentahapto coordination. The Ind hapticity in solution is also of interest and can be estimated from NMR data, as described in Section 3.1.

3. Group 10 metal indenyl complexes

This section describes the syntheses, structural features, and reactivities of Group 10 metal indenyl complexes, with $Ni(Ind)_2$ presented first and the complexes IndMLX and $[IndMLL']^+$ following thereafter. In order to facilitate the present discussion and also provide researchers in this field with a starting point in the literature search for Group 10 metal indenyl complexes, a list of all such compounds reported to date has been compiled in Table 2. This table contains the following information: (a) the Arabic numerals which will be used to refer to each compound throughout the remainder of this document; (b) the characterisation data available for each compound; and (c) the appropriate citation(s) for the primary literature reports.

3.1. $Ni(Ind)_2$

The Ind analogue of the well known nickelocene was first reported in 1969 by Köhler who described its preparation from $Ni(acac)_2$ and IndMgBr, and discussed its ^{1}H-NMR and mass spectra as well as its magnetic moment ($\mu = 1.05$ D) [25]. In a later report [26], Köhler presented an improved synthesis using IndLi, and proposed a method for extracting information on the M–Ind interaction (in solution) based on an analysis of the ^{13}C-NMR data. This method was based on the observation that the ^{13}C-NMR chemical shifts of C(3a) and C(7a), the ring junction carbon atoms in indene (Chart 1), move upfield upon coordination to metals. By examining the magnitude of this shift for various complexes, Köhler noted a correlation between the Ind ligand's (presumed) degree of hapticity in a given complex and the extent of the observed shift. For instance, the δ^{13}C(C3a/7a) for $Fe(Ind)_2$, which was presumed to have η^5-Ind ligands, showed an upfield shift of ca. 60 ppm in comparison to indene; the corresponding values for $[Co(Ind)_2]^+$ and $Ni(Ind)_2$ were ca. 45 and 10 ppm, respectively, reflecting the anticipated reduction in the hapticity of the Ind ligands on going from Fe to Co to Ni.

A variant of Köhler's NMR method measures the difference between Ind hapticities in $IndML_n$ and NaInd (as opposed to IndH), this method has been used by Baker and Marder to demonstrate a correlation between the solid state and solution hapticity of Ind ligands in a variety of complexes [27]. According to this method, the magnitude of the parameter $\Delta\delta^{13}C = \delta\{C(3a/7a)\text{ of M–Ind}\} - \delta\{C(3a/7a)\text{ of NaInd}\}$ reflects the solution hapticity of Ind in a given complex. For instance, the $\Delta\delta^{13}$C of +3.6 ppm for $Ni(Ind)_2$ is larger than the corresponding values for the complexes $Fe(Ind)_2$ (−43.7 ppm) and $[Co(Ind)_2]^+$ (−32.4 ppm) but smaller than the values in $(\eta^3\text{-Ind})Ir(PMe_2Ph)_3$ (+26 ppm) [28] and $[(\eta^3\text{-Ind})Fe(CO)_3]^-$ (+27 ppm) [29]. A report by Marder's group [27b] on the solid state structures of $Fe(Ind)_2$, $Fe(Me_7Ind)_2$, $Co(Ind)_2$, and $Ni(Ind)_2$ showed that the Ind hapticity in the solid state varies from a very nearly η^5 mode in $Fe(Ind)_2$ to an intermediate ($\eta^3 \leftrightarrow \eta^5$) mode in $Ni(Ind)_2$ (see the appropriate entries for $Fe(Ind)_2$ and $Co(Ind)_2$ in Table 1 and the entry for $Ni(Ind)_2$ in Table 3). Another difference among these complexes was that the Ind ligands adopt an eclipsed conformation in the $Fe(Ind)_2$ and $Co(Ind)_2$ but are staggered in $Ni(Ind)_2$, as illustrated in Fig. 1.

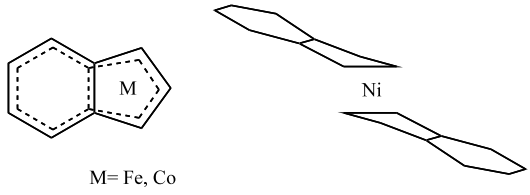

Fig. 1. Schematic drawings of the solid state structures of $M(Ind)_2$ showing the relative orientations of the Ind ligands (eclipsed when M = Fe and Co, staggered when M = Ni).

Table 2
Reported Group 10 metal Ind complexes

Complex	No.	Ref.	Characterisation
$Ni(Ind)_2$	**1**	[25,26,27b]	^1H, ^{13}C, UV–vis, X-ray
$Ni(1\text{-menthyl}–4,7\text{-}Me_2–Ind)_2$	**2a**	[7]	^1H, ^{13}C, IR, MS
$Ni(2\text{-}Ph–Ind)_2$	**2b**	[6]	X-ray
$IndNi(\eta^3\text{-allyl})$	**3**	[5]	^1H, ^{13}C
$R_n–IndNi(PPh_3)Cl$	**4**		
$R_n = H$	**4a**	[4a]	^1H, ^{13}C, ^{31}P, UV–vis, X-ray
1-Me	**4b**	[4c]	^1H, ^{13}C, ^{31}P, UV–vis, X-ray
1-Et	**4c**	[4q]	^1H, ^{13}C, ^{31}P
1-^iPr	**4d**	[4q]	^1H, ^{13}C, ^{31}P, X-ray
1-Bz	**4e**	[4q]	^1H, ^{13}C, ^{31}P
$1\text{-}SiMe_3$	**4f**	[4q]	^1H, ^{13}C, ^{31}P
$1\text{-}(CH_2)_2NMe_2$	**4g**	[4s]	^1H, ^{13}C, ^{31}P, X-ray
$1\text{-}(CH_2)_3NMe_2$	**4h**	[4h]	^1H, ^{13}C, ^{31}P
$1\text{-}(CH_2)_2N(^iPr)_2$	**4i**	[4n]	^1H, ^{13}C, ^{31}P
$1\text{-}(CH_2)_3NH(^tBu)$	**4j**	[4h]	^1H, ^{13}C, ^{31}P, X-ray
$1\text{-}(CH_2)_4NH(^tBu)$	**4k**	[4h]	^1H, ^{13}C, ^{31}P
$1\text{-}(2\text{-}CH_2–py)$	**4l**	[4n]	^1H, ^{13}C, ^{31}P, X-ray
1-{*N*-(CH_2CH_2)pyr[a]}	**4m**	[4n]	^1H, ^{13}C, ^{31}P
2-Me	**4n**	[4q]	^1H, ^{13}C, ^{31}P
2-Ph	**4o**	[4q]	^1H, ^{13}C, ^{31}P
$1,2\text{-}Me_2$	**4p**	[4q]	^1H, ^{13}C, ^{31}P
$1,3\text{-}Me_2$	**4q**	[4q]	^1H, ^{13}C, ^{31}P
$1,2,3,\text{-}Me_3–Ind$	**4r**	[4q]	^1H, ^{13}C, ^{31}P
$1,3\text{-}Me_2–2\text{-}Ph–Ind$	**4s**	[4q]	^1H, ^{13}C, ^{31}P, X-ray
$\{1\text{-}(CH_2)_2NMe_2–Ind\}Ni(PPh_3)I$	**4t**	[4j]	^1H, ^{13}C, ^{31}P, X-ray
$(1\text{-}Me–Ind)Ni(PPh_3)X$	**5**		
X = Br	**5a**	[4f]	^1H, ^{13}C, ^{31}P, X-ray
X = I	**5b**	[4f]	^1H, ^{13}C, ^{31}P
X = SMe	**5c**	[4l]	^1H, ^{31}P
X = SEt	**5d**	[4l]	^1H, ^{31}P
X = SPh	**5e**	[4l]	^1H, ^{13}C, ^{31}P, X-ray
$X = S(C_6F_5)$	**5f**	[4l]	^1H, ^{31}P, X-ray
$X = S(p\text{-}NO_2\text{-}Ph)$	**5g**	[4l]	^1H, ^{31}P, X-ray
X = phthalimide	**5h**	[4f]	^1H, ^{13}C, ^{31}P, X-ray
$X = 5,6\text{-}Cl_2–phthalimide$	**5i**	[4f]	^1H, ^{13}C, ^{31}P, X-ray
X = maleimide	**5j**	[4f]	^1H, ^{13}C, ^{31}P
X = succinimide	**5k**	[4f]	^1H, ^{13}C, ^{31}P
$(1\text{-}R–Ind)Ni(PPh_3)(OTf)$ [b]			
$R = {}^iPr$	**5l**	[4p]	^1H, ^{13}C, ^{31}P, X-ray
R = Et	**5m**	[4p]	^1H, ^{13}C, ^{31}P
R = Bz	**5n**	[4p]	^1H, ^{13}C, ^{31}P, X-ray
$R–IndNi(PMe_3)X$	**6**		
R = H, X = Cl	**6a**	[4a]	^1H, ^{13}C, ^{31}P
R = H, X = Me	**6b**	[4a]	^1H, ^{13}C, ^{31}P
R = 1-Me, X = Cl	**6c**	[4k]	^1H, ^{13}C, ^{31}P, X-ray
R = 1-Me, X = Me	**6d**	[4r]	^1H, ^{13}C, ^{31}P, X-ray
$R = {}^iPr$, X = Me	**6e**	[4o]	^1H, ^{13}C, ^{31}P, X-ray
$R = 1\text{-}(CH_2)_2NMe_2$, X = Cl	**6f**	[4n]	^1H, ^{13}C, ^{31}P, X-ray
$(1\text{-}Me–Ind)Ni(PCy_3)X$	**7**		
X = Cl	**7a**	[4k]	^1H, ^{13}C, ^{31}P, X-ray
X = Me	**7b**	[4r]	^1H, ^{13}C, ^{31}P, X-ray
X = CC–Ph	**7c**	[4g]	^1H, ^{13}C, ^{31}P, X-ray
$(1\text{-}Me–Ind)Ni(PR_3)Cl$	**8**		
R = Bu	**8a**	[4k]	^1H, ^{13}C, ^{31}P
$R = (CH_2)_2(CF_2)_6CF_3$	**8b**	[4k]	^1H, ^{13}C, ^{31}P, ^{19}F
$(1\text{-}Me–Ind)Ni(PPh_3)R$	**9**		
R = Me	**9a**	[4c]	^1H, ^{13}C, ^{31}P, X-ray
R = Et	**9b**	[4o]	^1H, ^{13}C, ^{31}P, X-ray

Table 2 (*Continued*)

Complex	No.	Ref.	Characterisation
R = *n*-Pr	**9c**	[4o]	^{1}H, ^{13}C, ^{31}P
R = ^{i}Pr	**9d**	[4o]	^{1}H, ^{13}C, ^{31}P
R = *n*-Bu	**9e**	[4o]	^{1}H, ^{13}C, ^{31}P
R = ^{i}Bu	**9f**	[4o]	^{1}H, ^{13}C, ^{31}P
R = *sec*-Bu	**9g**	[4o]	^{1}H, ^{13}C, ^{31}P
R = ^{t}Bu	**9h**	[4o]	^{1}H, ^{13}C, ^{31}P
R = Cy	**9i**	[4o]	^{1}H, ^{13}C, ^{31}P, X-ray
R = CH_2CMe_3	**9j**	[4o]	^{1}H, ^{13}C, ^{31}P, X-ray
R = CC–Ph	**9k**	[4g]	^{1}H, ^{13}C, ^{31}P, X-ray
R = CC–Bu	**9l**	[4g]	^{1}H, ^{13}C, ^{31}P
(1-R–Ind)Ni(PPh_3)(thienyl)	**10**		
R = Me	**10a**	[4t]	^{1}H, ^{13}C, ^{31}P, X-ray
R = Et	**10b**	[4t]	^{1}H, ^{13}C, ^{31}P, X-ray
R = ^{i}Pr	**10c**	[4t]	^{1}H, ^{13}C, ^{31}P
R = Bz	**10d**	[4t]	^{1}H, ^{13}C, ^{31}P
R = 1-Me–2-Ph	**10e**	[4t]	^{1}H, ^{13}C, ^{31}P, X-ray
(1-Me–Ind)Ni(L)Cl	**11**		
L = Imes[c]	**11a**	[4m]	^{1}H, ^{13}C, MS, X-ray
L = $ImesCl_2$[c]	**11b**	[4m]	^{1}H, ^{13}C, MS, X-ray
L = Ibut[c]	**11c**	[4m]	^{1}H, ^{13}C
L = Ipr[c]	**11d**	[4m]	^{1}H, ^{13}C, MS, X-ray
(1-Me–Ind)Ni(L)R	**12**		
L = Imes, R = Me	**12a**	[4m]	^{1}H, ^{13}C, MS, X-ray
L = Imes, R = CC–Ph	**12b**	[4m]	^{1}H, ^{13}C
L = $ImesCl_2$, R = Me	**12c**	[4m]	^{1}H, ^{13}C
$[(1\text{-Me–Ind})Ni(PMe_3)_2]^+$	**13**	[4o]	^{1}H, ^{13}C, ^{31}P, MS, X-ray
$[(1\text{-Me–Ind})Ni(PPh_3)_2]^+$	**14**	[4o]	^{1}H, ^{13}C, ^{31}P, MS, X-ray
$[(1\text{-Me–Ind})Ni(PPh_3)(PMe_3)]^+$	**15**	[4d]	^{1}H, ^{13}C, ^{31}P, X-ray
$[(1\text{-Me–Ind})Ni(dppe)]^+$	**16**	[4o]	^{1}H, ^{13}C, ^{31}P, MS, X-ray
$[(1\text{-Me–Ind})Ni(dppp)]^+$	**17**	[4o]	^{1}H, ^{13}C, ^{31}P, MS, X-ray
$[(1\text{-Me–Ind})Ni(dppf)]^+$	**18**	[4o]	^{1}H, ^{13}C, ^{31}P, MS, X-ray
$[(2\text{-Me–Ind})Ni(dippe)]^+$	**19**	[9]	^{1}H, ^{13}C, ^{31}P, MS, X-ray
$[(1\text{-}^{i}\text{Pr–Ind})Ni(PPh_3)L]^+$	**20**		
L = CO	**20a**	[4p]	^{1}H, ^{13}C, ^{31}P, IR
L = MeCN	**20b**	[4p]	^{1}H, ^{13}C, ^{31}P, IR, X-ray
L = CN(^{t}Bu)	**20c**	[4p]	^{1}H, ^{13}C, ^{31}P, IR, X-ray
L = py	**20d**	[4p]	^{1}H, ^{31}P
$[\{1\text{-}(CH_2)_2NMe_2\text{–Ind}\}Ni(dppe)]^+$	**21**	[4j]	^{1}H, ^{13}C, ^{31}P
$[\{1\text{-}(CH_2)_3NMe_2\text{–Ind}\}Ni(PPh_3)_2]^+$	**22**	[4j]	^{1}H, ^{13}C, ^{31}P
$[\{1\text{-}(CH_2)_3NH(^{t}Bu)\text{–Ind}\}Ni(PPh_3)_2]^+$	**23**	[4h]	^{1}H, ^{13}C, ^{31}P
$[\{1\text{-}(CH_2)_2NMe_2\text{–Ind}\}Ni(PPh_3)L]^+$	**24**		
L = PPh_3	**24a**	[4j]	^{1}H, ^{31}P
L = PMe_3	**24b**	[4j]	^{1}H, ^{31}P
L = py	**24c**	[4j]	^{1}H, ^{31}P
L = 2-Me–py	**24d**	[4j]	^{1}H, ^{31}P
L = 3-Me–py	**24e**	[4j]	^{1}H, ^{31}P
L = 4-Me–py	**24f**	[4j]	^{1}H, ^{31}P
L = 2,6-Me_2–py	**24g**	[4j]	^{1}H, ^{31}P
$[\{\eta^1,\eta^{3-5}\text{-}(CH_2)_2NMe_2\text{–Ind}\}Ni(PPh_3)]^+$	**25**	[4j]	^{1}H, ^{13}C, ^{31}P, X-ray
$\{1\text{-}(R\text{–}CMe_2)\text{–Ind}\}Ni(PPh_3)Cl$	**26**		
R = $CpNi(PPh_3)Cl$	**26a**	[8]	^{1}H, ^{13}C, ^{31}P
R = $[CpNi(PPh_3)_2]^+$	**26b**	[8]	^{1}H, ^{13}C, ^{31}P
$[\{1\text{-}(R\text{–}CMe_2)\text{–Ind}\}Ni(PPh_3)_2]^+$ R = $[CpNi(PPh_3)_2]^+$	**27**	[8]	^{1}H, ^{13}C, ^{31}P
1,1′-CMe_2–$\{[IndNi(PPh_3)_2]^+\}_2$	**28**	[8]	^{1}H, ^{13}C, ^{31}P
$\{IndPd(\mu\text{-Cl})\}_2$	**29**	[10]	^{1}H, ^{13}C, UV–vis
$IndPd(PMe_3)(CH_2SiMe_3)$	**30**	[13b]	^{1}H, ^{13}C, ^{31}P, X-ray
$[(R_n\text{-Ind})Pd(tmeda)]^+$	**31**	[12a]	
R_n = 1-Bz–4,5,6,-$(OMe)_3$	**31a**	[12a]	^{1}H, ^{13}C
1-Bz–3-Ph–4,5,6-$(OMe)_3$	**31b**	[12a]	^{1}H, ^{13}C, X-ray

Table 2 (*Continued*)

Complex	No.	Ref.	Characterisation
1-Bz–2,3-Ph_2–4,5,6-$(OMe)_3$	**31c**	[12a]	^1H, ^{13}C, X-ray
1-Bz–2,3-Me_2–4,5,6-$(OMe)_3$	**31d**	[12a]	^1H, ^{13}C
1-Bz–2-C(O)Me–4,5,6-$(OMe)_3$	**31e**	[12b]	^1H, ^{13}C, X-ray
1-Bz	**31f**	[12b]	^1H, ^{13}C
1-Bz–2,3-Me_2	**31g**	[12b]	^1H, ^{13}C
1-Bz–2,3-Et_2	**31h**	[12b]	^1H, ^{13}C, MS
1-Bz–2,3-Ph_2	**31i**	[12b]	^1H, ^{13}C
1-Bz–3-Ph	**31j**	[12b]	^1H, ^{13}C, MS, X-ray
1-Bz–2-Ph–3-Me	**31k**	[12b]	^1H, ^{13}C, MS
$[(R_n\text{-Ind})Pd(bipy)]^+$	**32**		
R_n = 1-Bz–2,3-Me_2–4,5,6,-$(OMe)_3$	**32a**	[12a]	^1H, ^{13}C
1-Bz	**32b**	[12b]	^1H, ^{13}C, MS
1-Bz–2,3-Me_2	**32c**	[12b]	^1H, ^{13}C, MS
1-Bz–2,3-Et_2	**32d**	[12b]	^1H, ^{13}C
1-Bz–2,3-Ph_2	**32e**	[12b]	^1H, ^{13}C
1-Bz–2(or 3)-Ph	**32f**	[12b]	^1H
1-Bz–2-Ph–3-Me	**32g**	[12b]	^1H, ^{13}C, X-ray
$\{(\mu\text{-Ind})Pd(CNR)\}_2$	**33**		
R = *t*-Bu	**33a**	[11]	^1H, ^{13}C, IR, UV–vis, X-ray
R = 2,6-$Me_2C_6H_3$	**33b**	[11]	^1H, ^{13}C, IR, UV–vis, X-ray
R = 2,4,6-$Me_3C_6H_2$	**33c**	[11]	^1H, ^{13}C, IR, UV–vis
R = 2,4,6-$^t Bu_3C_6H_2$	**33d**	[11]	^1H, ^{13}C, IR, UV–vis
$(\eta^1\text{-Ind})Pt(\eta^4\text{-COD})Cl$	**34**	[14]	^1H, ^{13}C
$(\eta^1\text{-Ind})_2Pt(\eta^4\text{-COD})$	**35**	[14]	^1H, ^{13}C
$[IndPt(COD)]^+$	**36**	[14]	^1H, ^{13}C

[a] pyr = pyrrolidine.
[b] OTf = OSO_2CF_3.
[c] Imes = (1,3-dimesityl)imidazol-2-ylidene; $ImesCl_2$ = (1,3-dimesityl)-4,5-dichloro-imidazol-2-ylidene; Ibut = (1,3-di-*t*-butyl)imidazol-2-ylidene; Ipr = (1,3-di-*i*-propyl)imidazol-2-ylidene.

An analysis of the X-ray and NMR results for the above complexes indicates that the $\Delta\delta^{13}C$ parameters reflect fairly accurately the solution hapticity of the Ind ligands which, in most cases, are very similar to the hapticities observed in the solid state. Thus, the Ind ligands are more or less pentahapto in $Fe(Ind)_2$ and $Co(Ind)_2$, essentially trihapto in $IndIr(PMe_2Ph)_3$ and $[IndFe(CO)_3]^-$, and of intermediate hapticity in $Ni(Ind)_2$. These results also support the notion that the number of valence electrons on the metal centre determines the extent of slip-fold distortions in the hapticity of Ind ligands [27b].

The latter point has been rationalised by an MO analysis reported in a recent theoretical treatment of bonding in Ind complexes [30]. The authors of this study argue, for instance, that going from $Fe(Ind)_2$ to $Ni(Ind)_2$ is tantamount to adding two extra electrons to the high-lying LUMO of $Fe(Ind)_2$ that has metal–indenyl antibonding character. The resulting destabilisation is minimised when the Ind ligands bend (or fold) and adopt a staggered conformation, as evident from the experimental data (Fig. 1). Taken together, these experimental and theoretical studies indicate that the Ni centre in $Ni(Ind)_2$ has a formal electron count of between 16 and 18 electrons; in other words, the flexible hapticity of the Ind ligands has allowed this complex to avoid the formal electron count of 20. This is in contrast to the situation in the analogous $NiCp_2$ wherein the extra pair of electrons (relative to ferrocene) are localised in the degenerate, antibonding ligand orbitals, leading to a nearly uniform lengthening of the Ni–C distances and rendering this compound paramagnetic [31]. The observation of a structure consisting of two equally slipped Ind ligands in $Ni(Ind)_2$ also contrasts with the presence of differently slipped Ind ligands, one almost fully η^3 and another almost fully η^5, in the complexes $(Ind)_2M(CO)_2$ (M = V [32], W [33]; see Table 1 for details).

The above data indicate that the ground state structures of nickelocene and $Ni(Ind)_2$ are quite different; in addition, there is some preliminary evidence showing that the excited states of these analogues are also different. For instance, the UV–visible spectrum of $Ni(Ind)_2$ shows an intense, broad absorption band (with a bandwidth of ca. 5000 cm^{-1}) in the green spectral region, with its maximum at 20 200 cm^{-1} (ca. 500 nm) and a molar absorptivity of 3180 M^{-1} cm^{-1} [4b]. In comparison, the lowest energy absorption band for nickelocene is in the red spectral region, with a maximum at 14 500 cm^{-1} (ca. 700 nm) and a molar absorptivity of 60 M^{-1} cm^{-1} [34]. Moreover, no luminescence is observed for $Ni(Ind)_2$ at temperatures

Table 3
Structural data on Group 10 metal Ind complexes

No.	M–C1 (Å)	M–C2 (Å)	M–C3 (Å)	M–C3a (Å)	M–C7a (Å)	ΔM–C (Å) [a]	HA (°) [a]	FA (°) [a]	$\Delta\delta^{13}C$ [b] (ppm)
1	2.068(3)	1.973(3)	2.056(3)	2.480(3)	2.483(3)	0.42	13.9	13.1	+3.6
4a	2.094(2)	2.061(2)	2.042(2)	2.318(2)	2.344(2)	0.26	10.9	11.7	ca. −2
4b	2.137(2)	2.072(2)	2.026(3)	2.308(2)	2.351(2)	0.25	11.0	11.8	ca. −2
4d	2.145(5)	2.048(5)	2.022(5)	2.329(4)	2.382(5)	0.27	11.0	10.5	–
4g	2.147(2)	2.071(2)	2.025(3)	2.314(3)	2.349(2)	0.24	8.9	9.2	
4j	2.135(6)	2.057(6)	2.028(6)	2.296(7)	2.357(8)	0.25	10.4	10.5	–
4l	2.132(3)	2.071(4)	2.037(4)	2.308(4)	2.352(3)	0.25	10.1	8.8	–
5e	2.113(5)	2.064(5)	2.058(5)	2.295(5)	2.328(5)	0.23	–	–	–
5f	2.160(3)	2.094(3)	2.031(3)	2.259(3)	2.313(3)	0.19	9.1	8.5	–
5g	2.149(10)	2.081(10)	2.044(11)	2.267(11)	2.315(10)	0.20	7.2	8.1	–
5h	2.118(5)	2.051(5)	2.025(5)	2.337(5)	2.341(5)	0.27	11.5	11.9	ca. −3
5l	2.131(2)	2.064(2)	2.024(2)	2.311(2)	2.335(2)	0.25	10.5	9.2	ca. −3
5n	2.171(3)	2.076(3)	2.018(3)	2.313(4)	2.360(3)	0.24	9.5	7.6	ca. −2
6c	2.1316(18)	2.0511(19)	2.0246(18)	2.3363(19)	2.3608(19)	0.27	11.5	–	ca. −2
6d	2.097(3)	2.076(3)	2.095(3)	2.298(3)	2.288(3)	0.20	8.4	7.0	ca. −8
6e	2.0987(19)	2.082(2)	2.075(2)	2.254(2)	2.270(2)	0.18	8.7	6.35	–
6f	2.1184(19)	2.0389(19)	2.0344(19)	2.3817(19)	2.4035(18)	0.32	12.5	13.2	ca. −1
7a	2.144(4)[c]	2.042(4)[c]	2.038(4)[c]	2.390(4)[c]	2.407(4)[c]	0.30	11.0	10.2	ca. −1
7b	2.104(4)	2.071(4)	2.110(4)	2.321(3)	2.320(3)	0.20	7.8	6.7	ca. −5
7c	2.092(3)	2.067(3)	2.079(3)	2.310(3)	2.293(3)	0.21	9.4	8.7	ca. −2
9a	2.089(4)	2.072(4)	2.082(4)	2.275(4)	2.273(4)	0.19	8.1	7.5	ca. −10
9b	2.096(2)	2.079(2)	2.107(2)	2.280(2)	2.269(2)	0.17	7.8	7.4	−9
9i	2.175(2)	2.094(2)	2.046(2)	2.233(2)	2.302(2)	0.16	6.9	5.9	−9
9j	2.120(3)	2.071(4)	2.125(3)	2.384(3)	2.364(4)	0.25	9.2	11.0	−5
9k	2.112(3)	2.088(3)	2.053(3)	2.276(4)	2.313(3)	0.21	10.2	12.0	–
10a	2.1058(17)	2.0742(17)	2.0709(18)	2.3066(17)	2.2924(17)	0.21	9.5	9.5	−12
10b	2.083(3)	2.073(3)	2.088(3)	2.303(3)	2.279(3)	0.21	9.2	8.4	−12
10e	2.0906(19)	2.0850(18)	2.0715(19)	2.2893(19)	2.286(2)	0.21	10.1	10.8	−12
11a	2.157(3)	2.033(4)	2.014(3)	2.385(3)	2.426(3)	0.32	11.8	10.6	ca. 0
11b	2.156(3)	2.036(4)	2.038(3)	2.423(3)	2.458(3)	0.34	12.2	12.3	+2
11d	2.139(2)	2.039(2)	2.028(2)	2.385(2)	2.423(2)	0.32	12.1	9.7	+4
12a	2.108(2)	2.061(3)	2.119(2)	2.370(3)	2.350(2)	0.25	8.9	8.9	ca −8
13	2.188(13)	1.984(16)	2.025(14)	2.222(13)	2.289(13)	0.15	5.6	2.8	ca. −6
14	2.153(9)	2.038(10)	2.097(9)	2.375(10)	2.405(9)	0.27	3.8	5.7	ca. −7
15	2.160(2)	2.096(2)	2.033(2)	2.249(2)	2.305(2)	0.18	–	–	–
17	2.166(2)	2.088(2)	2.038(2)	2.276(2)	2.340(2)	0.21	9.5	11.8	ca. −9
19	2.092(9)	2.066(9)	2.03(1)	2.298(9)	2.30(1)	0.24	10.3	10.0	ca. −8
20b	2.128(2)	2.064(2)	2.013(2)	2.283(2)	2.326(2)	0.23	10.6	8.1	ca. −5
20c	2.082(3)	2.066(3)	2.038(3)	2.248(3)	2.248(3)	0.19	10.1	7.7	ca. −8
25	2.040(2)	2.056(3)	2.078(3)	2.327(3)	2.314(2)	0.26	11.8	9.3	ca. −1
30	2.346(5)	2.217(5)	2.267(6)	2.659(5)	2.724(5)	0.39	–	12.4	+5
31b	2.253(4)	2.187(5)	2.191(4)	2.585(5)	2.565(4)	0.35	–	–	–
31c	2.208(5)	2.151(5)	2.212(6)	2.572(5)	2.564(4)	0.36	–	–	–
31e	2.185(4)	2.175(4)	2.220(4)	2.567(4)	2.547(4)	0.36	–	11.2	–
31j	2.204(5)	2.157(6)	2.244(5)	2.603 [e]	2.603 [e]	0.41	–	17.7	–
32g	2.211(3)	2.167(4)	–	2.630[e]	2.630[e]	0.42	–	14.5	–
33a[d]	2.17(2), 2.20(2)	2.43–2.48	2.20(2), 2.19(2)	3.05(2), 3.07(2)	3.13(2), 3.07(1)	0.90	–	10.3	−8
33b[d]	2.16(1), 2.17(2)	2.49–2.52	2.19(1), 2.18(2)	3.01(1), 3.00(1)	2.99(1), 3.03(2)	0.83	–	6.5	−7

[a] Definitions given in Table 1 footnotes.
[b] $\Delta\delta^{13}C = \delta$ {C(3a/7a) of M–Ind} $-\delta$ {C(3a/7a) of Na^+Ind^-}.
[c] Average of the values for the two molecules in the unit cell.
[d] In these complexes there are two Pd centres positioned between the two Ind ligands. The bond lengths given are as follows: for M–C1 and M–C3, the distances from each Pd to the two C atoms (one from each Ind) closest to it; for M–C2, the range of all four Pd–C2 bond lengths; for M–C3a and M–C7a, the distances from each Pd to the two ring junction C atoms (one from each Ind) closest to it. The slip parameters are averaged over all values.
[e] Average values for Pd–C3a and Pd–C7a distances.

greater than 5 K, whereas nickelocene shows weak, near-infrared luminescence under the same conditions [4b].

Before ending this discussion, it is worth noting that no reactivity studies have been reported for $Ni(Ind)_2$ in contrast to the relatively well-studied reactivities of

nickelocene [35]. Moreover, the corresponding bis(indenyl) complexes of Pd and Pt have not been reported yet. Thus, many aspects of the chemistry of $M(Ind)_2$ are yet to be uncovered. Similarly, little is known about the structures and reactivities of $Ni(Ind)_2$ derivatives bearing substituted Ind ligands. Recently, Schumann et al. have reported that all three possible diastereomers of the complex (1-{(−)-3-menthyl}-4,7-Me_2–$Ind)_2Ni$ can be obtained upon reacting $NiCl_2 \cdot DME$ with the lithium salt of the corresponding indenyl ligand [7]; the separation and isolation of the individual diastereomers has not been achieved. The attempted syntheses of Ni(1-R–$Ind)_2$ bearing achiral substituents (e.g. Ni(1-Me–$Ind)_2$) have also given complex mixtures of products [4l]. As a result, no structural information is available to date for $Ni(Ind)_2$ compounds bearing unsymmetrically substituted Ind ligands. On the other hand, the complex Ni(2-Ph–$Ind)_2$ and the related compounds $[Cp^*Ni(\mu,\eta,\eta$-indacenyl)$NiCp^*]^{n+}$ ($n = 0$, 2) [36] have been structurally characterised.

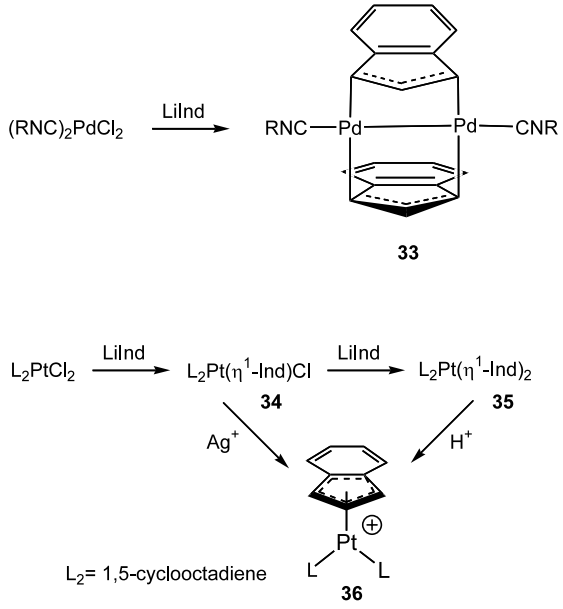

Scheme 4.

3.2. *IndM(L)(X) and [IndMLL′]+*

3.2.1. *Synthesis*

The main synthetic pathways to the complexes IndMLX involve the metathetic reactions of M′Ind (M′ = Li, Na, K, or MgX) with the metal halide salts followed by ligand exchange reactions of the complexes thus obtained (Scheme 3). Many complexes comprising different L and X ligands have been prepared in this manner, in addition to compounds in which both L and X are incorporated in one ligand such as $IndNi(\eta^3$-allyl) and $\{IndPd(\mu$-$Cl)\}_2$ (Scheme 3).

Although the metathetic procedures yield the desired products in most cases, unexpected side reactions have been reported with some dihalide precursors. For example, the reaction of $(RNC)_2PdCl_2$ with LiInd leads to the Pd(I) species $\{(\mu,\eta^3$-Ind)Pd(RNC)$\}_2$ [11], the only Group 10 Ind derivatives in which the metal centre is not in the oxidation state of +2 (Scheme 4). On the other hand, the reaction of $(COD)PtCl_2$ (COD = 1,4-cyclooctadiene) with NaInd gives the η^1-Ind derivatives $(COD)Pt(\eta^1$-Ind)Cl or $(COD)Pt(\eta^1$-$Ind)_2$, depending on the Pt:Ind ratio used (Scheme 4) [14]. The unexpected preference in this complex for η^1- as opposed to $\eta^5 \leftrightarrow \eta^3$-Ind is presumably related to the fact that the

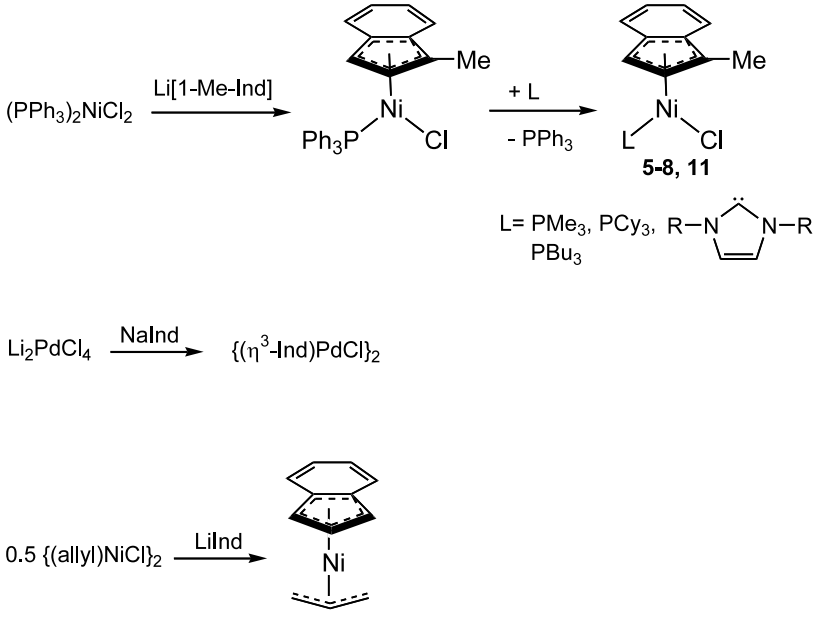

Scheme 3.

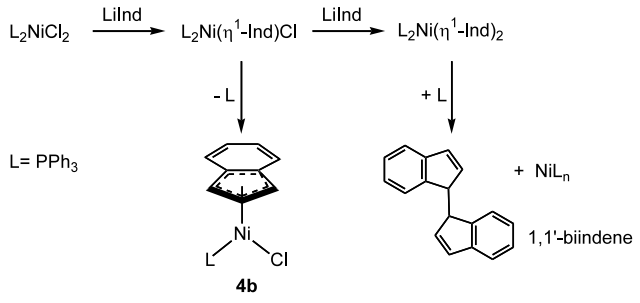

Scheme 5.

chelating COD ligand prevents the opening of a coordination site around the metal centre, thereby hindering the $\eta^1 \rightarrow \eta^5$ isomerisation. Interestingly, the analogous reaction with NaCp* gives the complex $[\eta^5$-Cp*Pt(COD)$]^+$ as the initial product; further reaction with a second equivalent of NaCp* gives the ultimate product, η^5-Cp*Pt$\{\eta^1,\eta^2$-(C_8H_{12})Cp*$\}$, in which a Cp* has been added to one C–C double bond of COD [14].

In the case of precursors such as $(PPh_3)_2NiCl_2$, a different side reaction arises from the well known ability of these complexes to act as coupling catalysts for organic anions. Thus, the reaction of this precursor with Ind anions produces variable amounts of the indenyl homocoupling products 1,1′-biindenes (Scheme 5) [4a]. This undesirable side reaction is thought to be caused by the slow dissociation of one of the PPh_3 ligands, which hampers the conversion of the initially produced η^1-Ind species to the desired η-IndNi(PPh_3)Cl. The coupling product is presumably formed by the coordination of the second η^1-Ind to give the postulated intermediate $(PPh_3)_2$Ni$(\eta^1$-Ind$)_2$, followed by reductive elimination. Consistent with this scenario, this side reaction can be avoided or minimised by following a number of preventive measures aimed at blocking the formation of $(PPh_3)_2$Ni$(\eta^1$-Ind$)_2$. These measures include: (a) the use of Ind ligands substituted at the C1 (or C3) position, (b) doing the synthesis at ambient or higher reaction temperatures over relatively short reaction times, (c) keeping the precursors $L_n NiX_2$ in excess, and (d) using Li^+ salts of Ind in preference over other salts. Another effective strategy is to block the entry of a second equivalent of Ind^- by using the monohalide precursors L_nMRX; the corresponding derivatives IndMLR (M = Ni [4o], Pd [13b]) can thus be obtained in better yields (Scheme 6).

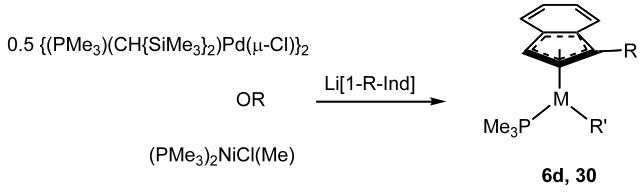

Scheme 6.

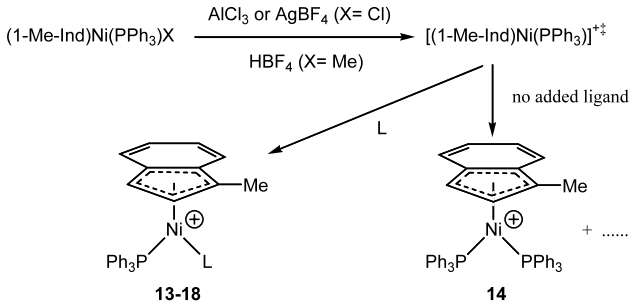

Scheme 7.

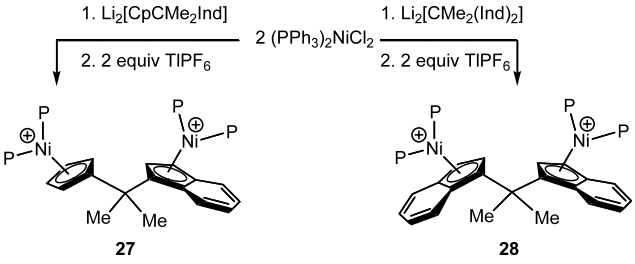

Scheme 8.

The cationic complexes $[IndMLL']^+$ are commonly prepared by abstracting the X ligand from IndMLX or by protonating the R ligand in IndMLR (Scheme 7). This strategy has been employed to prepare a novel series of bimetallic Ni complexes bearing two Ind or mixed Ind/Cp ligands (Scheme 8) [8]. These reactions are believed to proceed by the generation of the coordinatively and electronically unsaturated, cationic intermediate $[IndML]^+$ that can be trapped by the added ligand L′. It has been shown [4d] that if these Ni cations are generated in the absence of an added ligand, the highly electrophilic intermediate (the so-called "naked" cation $[IndNiL]^+$) abstracts another L from the reaction medium (probably from an unreacted IndNiLX) to give $[IndNiL_2]^+$ in poor yields (Scheme 7).

In the case of the Pt complexes discussed earlier, protonation of one of the σ-Ind ligands leads to the cationic η-Ind derivative (Scheme 4) [14], while the first and only cationic Pd(II) complexes reported to date have been prepared by a novel procedure involving multiple insertion reactions into Pd–C and Pd–H bonds (Scheme 9) [12]. If proven to be general, the latter approach offers a potentially attractive route to Group

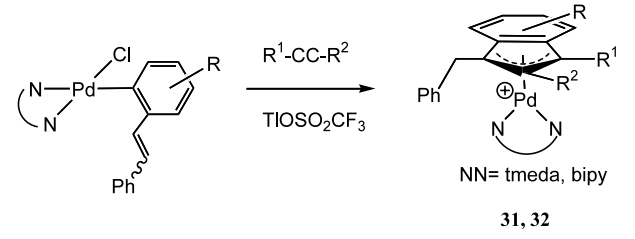

Scheme 9.

10 metal complexes bearing highly substituted Ind ligands.

3.2.2. Structural features

As expected on the basis of their d^8 configuration, most Group 10 metal Ind complexes reported to date adopt variously distorted square planar geometries in the solid state, and their colours range from different shades of red to orange–yellow. Thus, most of the neutral Ni complexes are reddish except for the thiolato complexes (1-Me–Ind)(PPh_3)Ni–SR (R = Ar, Me, Et), which are green or brown depending on the crystallisation conditions [4l]; on the other hand, the cationic Ni complexes and most Pd and Pt complexes are yellowish.

The few reported UV–visible studies of the neutral complexes have shown that their electronic structures are typical of other d^8 compounds in that they possess two absorption bands in the visible region of the spectrum (ca. 600–400 nm). EHMO calculations on the Ni complexes (1-Me–Ind)(PPh_3)Ni–Cl and (1-Me–Ind)(PPh_3)Ni–Me point to HOMO–LUMO gaps of ca. 20 000 cm^{-1} (2.5 eV) and 22 000 cm^{-1} (2.7 eV), respectively [4b]. Similar calculations on IndPd(acac), which is yet to be prepared experimentally, showed a smaller HOMO–LUMO gap of ca. 1.5 eV [10].

Table 3 lists the main bonding parameters for the structurally characterised examples of complexes IndMLX; these parameters, and in particular the ΔM–C values, are useful for developing a sense of the bonding picture in these complexes. An inspection of the data in Table 3 indicates that many factors influence the value of the ΔM–C parameter, including the nature of the ligands X and L. In cationic complexes, the substituents on Ind also play an important role in determining the Ind hapticity. The complexes (R_n–Ind)Ni(L)(X) and [(R_n–Ind)NiLL′]$^+$ constitute an extensive series in terms of different R, L, and X; a structural analysis of these complexes is presented below to illustrate how the various components of each complex and its overall charge can bring about different structural features.

3.2.2.1. (R_n–Ind)Ni(L)(X). The compound Ind-Ni(PPh_3)Cl (**4a**), displays a ΔM–C value of 0.26 Å, a HA of ca. 11°, and a FA of ca. 12°, indicating that the slip-fold distortion in this complex is less pronounced than that found in $Ni(Ind)_2$. This is presumably because η^5-Ind ligands would lead to a 20 electron configuration in $Ni(Ind)_2$ but only an 18 electron configuration in Ind$Ni(PPh_3)$Cl. Structural studies of other members of this series of complexes have shown little or no effect on the Ind hapticity as a function of Ind substituents, but the available data has underlined the importance of X and L ligands in this regard. For instance, complex **4b**, the 1-Me–Ind analogue of **4a**, displays essentially the same hapticity pattern as its parent compound; on the other hand, the Ni–Me analogue, **9a**, shows a lower degree of slip-fold distortions (ΔM–C ca. 0.19 Å, HA and FA ca. 8°). In general, with L = PPh_3, the ΔM–C values increase in the order X = Et (**9b**, 0.17 Å), Me (**9a**, 0.19 Å), CC–Ph and thienyl (**7c**, **9k**, and **10**, 0.21 Å), SPh (**5e**, 0.23 Å), Cl (**4a**, 0.26 Å), and phthalimide (**5h**, 0.27 Å). With X = Cl, on the other hand, the ΔM–C values increase in the order L = PPh_3 (**4b**, 0.25 Å), PMe_3 (**6c**, 0.27 Å), PCy_3 (**7a**, 0.30 Å), Imes[4] (**11a**, 0.32 Å), and $ImesCl_2$[5] (**11b**, 0.34 Å).

While more data is necessary to establish clear correlations between the slip-fold distortions of the Ind ligand in these complexes and the specific characteristics of the ligands L and X, the following trends emerge from the results cited above:

(i) For a given L (e.g. PPh_3), ligands such as alkyl, alkenyl, and alkynyl (i.e. effective σ donors with strong *trans* influence values) cause the least slippage (ΔM–C < 0.21 Å), while heteroatom-based ligands such as Cl (i.e. potentially π donating, relatively poor σ donors with weak *trans* influences) cause greater slippage (ΔM–C ~ 0.25 Å).
(ii) For a given X (e.g. Cl or Me), the more basic the L ligand, the higher the ΔM–C value (compare: **4b** vs. **6c** vs. **7a** vs. **11a**; **9a** vs. **6d** vs. **7b** vs. **12a**,**b**).

Structural studies of IndNiLX complexes have also revealed an unsymmetrical bonding mode for the Ind ligand in some of these complexes, as seen from the M–C1 vs. M–C3 distances listed in Table 3. For example, Ni–C1 is longer than Ni–C3 in complexes **4a**, **4b**, **5h**, **5l**, **6c**, **7a**, **11a**, and **11b**. When the difference in the M–C distances to the carbons on either side of the C_2 axis is significant, it can be argued that the distortion in the hapticity of the Ind is not quite $\eta^5 \leftrightarrow \eta^3$ but rather $\eta^5 \leftrightarrow (\eta^1,\eta^2)$ (Chart 2). This argument is particularly convincing in complexes wherein the corresponding C–C distances within the Ind ligand are consistent with a

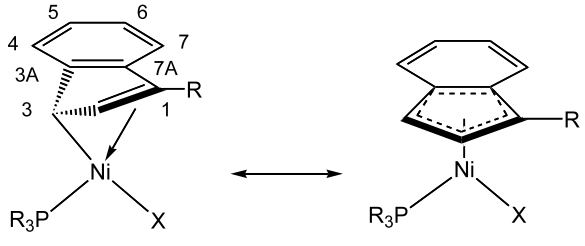

Chart 2.

[4] Imes = (1,3-dimesityl)imidazol-2-ylidene.
[5] $ImesCl_2$ = (1,3-dimesityl)-4,5-dichloroimidazol-2-ylidene.

localised allylic distortion. For instance, in the complexes **5n** and **11a**, the distances Ni–C3 versus Ni–C1 and C1–C2 versus C2–C3 are sufficiently different to warrant characterisation of the bonding as localised (η^1,η^2-Ind): in **5n**, Ni–C3 = 2.018(3) Å < Ni–C1 = 2.171(3) Å and C1–C2 = 1.392(5) Å < C2–C3 = 1.435(5) Å; in **11a**, Ni–C3 = 2.014(3) Å < Ni–C1 = 2.157(3) Å and C1–C2 = 1.380(5) Å < C2–C3 = 1.418(5) Å. In contrast, complexes **6d**, **7b**, **9a**,**b**, and **12a**,**b** exemplify the cases wherein the Ni–Ind interaction is essentially symmetrical (Ni–C1 ≈ Ni–C3 and Ni–C3a ≈ Ni–C7a) and the bonding in the allylic moiety of the Ind ligands is delocalised. It has been argued that the asymmetry in the Ni–C1 and Ni–C3 bond distances is related to the relative *trans* influences of the L and X ligands [4c], although other factors are also involved (vide infra).

An important question which arises is whether the bonding features observed in the solid state structures of these complexes are maintained in solution; this question is relevant since the reactivities of these complexes are expected to be influenced by the solution hapticity of the Ind. The chemical shifts for the symmetry related protons H1/H3 and carbons C1/C3 can be used to extract information about the hybridisation of C1 and C3 carbons, and hence the type of interactions they have with the Ni centre. Thus, the low temperature δ values for H1/H3 in IndNi(PMe_3)Cl (**6a**) are more than 2 ppm apart (δH1 > δH3), attesting to the greater sp^2 character of C1. This difference is even larger (> 2.9 ppm) for H1/H3 signals in the PPh_3 analogue **4a** mainly because of the ring current effects of the phenyl groups which lie below H3. In the latter complex, the δ^{13}C values are more than 20 ppm apart (C1 more downfield). These data support the notion that the unsymmetrical hapticity of Ind observed in the solid state is also maintained in the solution.

An interesting consequence of the unsymmetrical M–Ind interaction in solution is the significantly hindered rotation of the Ind ligand about the M–Ind axis. In the complex **4a**, for instance, the energy barrier to the Ind rotation is ca. 16 kcal mol^{-1}; in comparison, the corresponding energy barrier in the complex IndNi(PPh_3)Me which has a symmetrical Ni–Ind bonding is ca. 10 kcal mol^{-1}. When these values are compared to the corresponding energy barriers in the complexes (2-Ph–Ind)Ni(PPh_3)Cl (16.5 kcal mol^{-1}), (1,3-Me_2–Ind)Ni(PPh_3)Cl (15.6 kcal mol^{-1}), and (1,3-Me_2–2-Ph–Ind)Ni(PPh_3)Cl (> 16.9 kcal mol^{-1}) it becomes evident that the steric factors are relatively less important than the hapticity of the Ind (i.e. the degree of slippage) in determining the ease with which the Ind ligand rotates about the metal centre.

As stated earlier, another method for determining the solution hapticity of Ind ligands is by means of the $\Delta\delta^{13}$C values; an analysis of these values for the above complexes supports the supposition that the solid state hapticity is maintained in solution. For instance, the $\Delta\delta^{13}$C values for the Ni–Cl derivatives **4a**, **4b**, **6c**, and **7a** are around −2 ppm (Table 3), indicative of an intermediate $\eta^5 \leftrightarrow \eta^3$ hapticity; on the other hand, the Ni–Me derivatives **6d** (−8 ppm), **9a** (−10 ppm), and **12a** (−8 ppm) possess more negative $\Delta\delta^{13}$C values consistent with smaller slippage values. Although there appears to be some degree of correlation between the solid state and solution hapticities in most cases (i.e. the larger the ΔM–C the more positive the $\Delta\delta^{13}$C), no strong relationship exists over the entire range of the Group 10 metal Ind complexes considered here. One possible reason for this weak correlation is the fact that the $\Delta\delta^{13}$C values examined here have not been obtained under a uniform set of conditions (solvent, temperature, etc.).

3.2.2.2. [(R$_n$–Ind)NiLL′]$^+$. The positive charge on cationic complexes would be expected to increase the electrophilicity of the metal centre and result in a stronger M–Ind interaction (i.e. less pronounced slippage). This appears to be the case for some of the complexes having ΔM–C values of 0.15–0.20 Å, but in some other complexes the slippage parameters are similar to those found for the neutral complexes (ΔM–C ca. 0.23–0.27 Å).

An important factor that affects the extent of slippage in these complexes appears to be the steric environment around the metal. This is evident from a comparison of the ΔM–C values for [(1-Me–Ind)Ni(PPh_3)$_2$]$^+$ (**14**, 0.27 Å), [(1-Me–Ind)Ni(PPh_3)(PMe_3)]$^+$ (**15**, 0.18 Å), and [(1-Me–Ind)Ni(PMe_3)$_2$]$^+$ (**13**, 0.15 Å). These observations seem to suggest that the larger steric bulk of the PPh_3 ligand might be the cause of the larger slippage in **14**; if the donor power of the phosphines were crucial, we would anticipate the opposite order of slip-fold distortions because the more basic PMe_3 would be expected to cause more slippage. In addition, the smaller slippage in the complex [(1-Me–Ind)Ni(dppp)]$^+$ (**17**, 0.21 Å) compared to **14** is consistent with the smaller cone angle of dppp due to chelation. It should be noted, however, that in some cases the influence of the steric factors is not as important as the electronic factors. This can be seen from a comparison of the slippage values in the complexes [(1-^{i}Pr–Ind)Ni(PPh_3){CN(^{t}Bu)}]$^+$ (**20c**, 0.17 Å) and [(1-^{i}Pr–Ind)Ni–(PPh_3)(NCMe)]$^+$ (**20b**, 0.23 Å); the greater π-accepting nature of RNC versus RCN is presumably the cause of the unusually small slippage in **20c**.

An unexpected finding from the structural studies of the cationic complexes concerns the symmetry of the Ni–C bonds. Recall that in the case of neutral species it was found that the relative σ-donating strengths of the ligands L and X determined whether the Ni–Ind interaction was symmetrical or not. By analogy, it would be expected that when L and L′ are similar

ligands, the Ni–Ind interaction in $[IndNiLL']^+$ should be symmetrical (i.e. Ni–C1 should be fairly equal to Ni–C3). Inspection of the Ni–C1 and Ni–C3 bond lengths for complexes **13**, **14**, **17**, and **19** shows that this is not the case. Indeed, the two Ni–P bond lengths are also somewhat unequal in **13** (2.203(5) vs. 2.144(4) Å), **14** (2.231(3) vs. 2.191(3) Å), and **19** (2.174(3) vs. 2.153(3) Å). In the case of **13** and **14**, the phosphine ligand on the side of the Me substituent is farther away from the Ni and seems to exert a weaker *trans* influence. It appears, therefore, that the steric factors influence the two Ni–PR_3 distances such that one ligand ends up exerting a greater net *trans* influence than the other, as evident from the unequal Ni–C1 and Ni–C3 bond lengths. One case in which the inverse correlation is observed between *trans* influence and Ni–C bond lengths is complex **25**. The geometrical constraints introduced by the chelating tether moiety in this compound result in a Ni–C1 bond length which is shorter than that of Ni–C3; this is opposite of what would be expected on the basis of the relatively stronger *trans* influence of PPh_3.

As was the case with the neutral complexes discussed above, the solution hapticity of the cationic complexes shows some correlation with the slippage values obtained from solid state structural data. In general, the cations show $\Delta\delta^{13}C$ values of ca. −5 to −10 ppm, which are similar to those of neutral Ni–Me derivatives. Moreover, the unsymmetrical Ni–Ind interaction in the cations is reflected in the ^{1}H-NMR chemical shift of H3, as follows. As indicated earlier, an upfield value for the chemical shift of the H3 signal indicates an increasingly unsymmetrical Ind hapticity caused by the relatively weak *trans* influence of the ligand X in $IndNi(PPh_3)X$. Similarly, the relative *trans* influence of the ligand L in $[IndNi(PPh_3)L]^+$ can be inferred from the chemical shift of H3 in these complexes. Thus, comparison of the H3 chemical shifts in the series of complexes $[(1\text{-}^i Pr\text{–}Ind)Ni(PPh_3)L]^+$ leads to the following *trans* influence order for the ligands L (δ ^{1}H for H3): CO (5.53 ppm) > PPh_3 (5.13 ppm) > CN(^{t}Bu) (4.80) > PhCN (4.30 ppm) > Py (4.21 ppm) ~ MeCN (4.18 ppm) [4p].

Finally, the Ind hapticity in the cationic complexes is also reflected in the size of the energy barrier for the rotation of the Ind about the Ni–Ind axis. Recall that the absence of a C2 axis in $[(1\text{-Me–Ind})Ni(PR_3)_2]^+$ renders the two P nuclei inequivalent and so studying the $^{31}P\{^1H\}$-NMR spectrum of this complex as a function of temperature yields the energy barrier for the Ind rotation. As an example, a barrier of 14.3 kcal mol^{-1} has been obtained for the rotation of the Ind in complex **16** [4o].

3.2.2.3. $IndPdL_n$ and $[IndPdL_2]^+$. Only one neutral [13b] and five cationic [12] Pd(II) complexes have been structurally characterised to date. The ΔM–C value of 0.39 Å found in the neutral complex **30** is much larger than the corresponding values in the analogous Ni–alkyl complexes. In addition, the Pd–Ind bonding is fairly unsymmetrical, implying a larger *trans* influence for the $CH(SiMe_3)_2$ ligand relative to PMe_3. Consistent with this unsymmetrical interaction, the rotation of the Ind ligand in **30** is relatively hindered ($\Delta G^{\ddagger}$ ca. 12.3 kcal mol^{-1}). This rotational energy barrier is higher than the corresponding value in $IndNi(PPh_3)Me$ (10.1 kcal mol^{-1}) but less than that in $IndNi(PPh_3)Cl$ (15.6 kcal mol^{-1}), even though the Ind ligand has a lower hapticity in the Pd complex than in both of these Ni complexes. This seemingly anomalous observation might be due to the significantly longer Pd–Ind versus Ni–Ind distances.

The cationic Pd(II) complexes **31** and **32** display slippage values which are very similar to the corresponding values for the neutral complex **30**. Although the Pd–C bonds are unsymmetrical in most cases except in **31c**, the Pd–C1 and Pd–C3 bond lengths are more similar in **31** and **32** than in the cationic Ni complexes discussed earlier. It is too early to tell whether the greater slippage in these Pd complexes compared to the corresponding Ni complexes will result in greater reactivities; there is, however, some indication already that the Ind ligand in **30** is prone to insertion reactions (vide infra).

The Pd(I) bimetallic complexes **33b** and **33c** show novel metal–Ind interactions [11], as follows. The two Ind ligands face each other in a wedge arrangement that results in a *syn* disposition of the two 6-membered moieties; the dihedral angle between the two Ind ligands is 66.5 and 48.3° in the two structures studied. The Ind ligands thus bridge the two Pd(I) centres, which are bonded to each other to give a diamagnetic complex. The coordination sphere of each Pd atom is completed by an isonitrile ligand. The distances from the Pd centres to the closest ring junction carbon atoms (3.00–3.13 Å) are outside normal bonding range, and the ΔM–C values of 0.8–0.9 Å indicate that the hapticity of both Ind ligands is η^3. The low hapticity of the Ind ligands in these complexes can be understood in light of the 12-electron configuration of each Pd centre in the $[Pd_2L_2]^{2+}$ unit; the contribution of 4 electrons from each Ind results in 16 valence electrons for each Pd centre (total of 30 electrons in the dimer).

No X-ray diffraction studies have been reported on Pt–Ind complexes.

3.2.3. Reactivities

Most of the reactivity studies reported to date for Group 10 metal Ind complexes involve the complexes IndNiLX and $[IndNiLL']^+$; these are described in Sections 3.2.3.1 and 3.2.3.2. The few reactions reported for Pd–Ind have been summarised below.

Reacting the Pd(I) complexes **33** with acetic acid results in the protonation of the μ-Ind ligands and the formation of the tetranuclear Pd(I) cluster $Pd_4(\mu,\eta^2$-

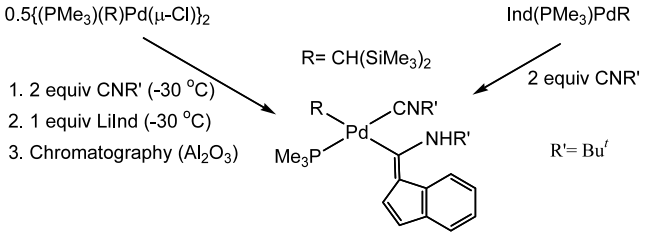

Scheme 10.

OAc)$_4$(μ,η^1-RNC)$_4$ [11]. The solid state structure of this cluster shows that the four Pd atoms lie in a rectangular array with two short and two long Pd–Pd bonds (ave. 2.650 and 2.894 Å, respectively); the short Pd–Pd bonds are bridged by nearly linear isocyanides, whereas the long Pd–Pd bonds are bridged by the acetate ligands.

The Pd(II) complex **30** reacts with 2 equiv. of :CNR (R = ^{t}Bu) to give an indenylfulvene complex in ca. 40% yield along with a number of unidentified products (Scheme 10) [13a]. Carrying out this reaction at low temperature and with only one equiv. of :CNR has allowed the detection of an intermediate bearing an η^1-Ind ligand; in the presence of another equivalent of :CNR and at temperatures above 0 °C the η^1-Ind inserts into the Pd–CNR bond to give the indenylfulvene product. Interestingly, this same product can also be accessed by the sequential reactions of the precursor {(CHSiMe$_3$)Pd(PMe$_3$)(μ-Cl)}$_2$ with 2 equiv. of :CNR and 1 equiv. of IndLi at −30 °C [13a]. It is not clear whether the latter reaction goes through the η^1-Ind intermediate detected in the previous reaction or via an outer sphere, nucleophilic attack by LiInd on a coordinated :CNR.

3.2.3.1. Reactivities of IndNiLX. The reactivities of these complexes are somewhat limited by their inertness towards insertion reactions. Thus, the derivatives with X = alkyl, alkenyl, alkynyl, thiolate, and imidate do not react with olefins, alkynes, and ketones in the absence of activators. However, the Ni–Me derivatives react readily with PhSiH$_3$, and this reaction forms the basis for a new catalytic system for the polymerisation of silanes. Olefin or alkyne polymerisations are also catalysed by the Ni–Cl, Ni–alkyl, Ni–alkenyl, and Ni–alkynyl derivatives when an appropriate co-catalyst/activator such as poly(methylaluminoxane) (PMAO) is present in excess. A brief summary of the scope of these reactions is given below. The derivatives with X = triflate are good precursors for the in-situ formation of the cationic species [IndNiL]$^+$ that promote alkene oligo- and polymerisations; these reactions are described in Section 3.2.3.2.

3.2.3.1.1. Si–H activation reactions. The combination of IndNi(PPh$_3$)Cl and PMAO gives a mixture of species which react with a large excess of PhSiH$_3$ to produce linear and cyclic polysilanes (PhSiH)$_n$. The linear portion of these polymers have M_w in the range of 2–7×10^3 and relatively narrow polydispersities (M_w/M_n ca. 2) [4e]. This system was initially thought to operate via a cationic mechanism involving an intermediate of the type [(1-Me–Ind)Ni(PPh$_3$)]$^+$; later studies indicated, however, that the catalysis is initiated primarily by neutral Ni–Me derivatives formed in-situ by the methylation of the Ni–Cl precursor with PMAO. Indeed, the direct reaction of PhSiH$_3$ with the Ni–Me derivatives in the absence of PMAO results in the evolution of CH$_4$ (initially) and H$_2$ (subsequently), and produces varying mixtures of cyclic and linear oligosilanes (PhSiH)$_n$ with $n = 5$–16 [4r]. It is noteworthy that the oligosilanes obtained from this system display relatively high molecular weights and narrow polydispersities (M_w/M_n ca. 1.1–1.5) in contrast to the majority of the previously reported late metal systems which produce only short oligomers (mainly dimers and trimers) [37]. However, the chain lengths produced by these Ni indenyl complexes are still much shorter than those obtained from some of the best early metal systems such as (Cp)(Cp*)ZrCl$_2$/^{n}BuLi/B(C$_6$F$_5$)$_3$ ($M_w \sim 3000$–14 000, $M_w/M_n > 2$) [38].

Kinetic studies of the reaction taking place between (1-Me–Ind)Ni(PMe$_3$)Me and PhSiH$_3$ have allowed the determination of the following kinetic parameters: $\Delta H^{\ddagger} = 10.7 \pm 0.7$ kcal mol^{-1} and $\Delta S^{\ddagger} = -42 \pm 2$ eu [4r]. The relatively large negative value of $\Delta S^{\ddagger}$ implies a highly ordered transition state for the reaction under study, and is consistent with the coordination of the Si–H bond to the Ni centre prior to the activation step. Consistent with this scenario, the initial reaction rate is highly dependent on the steric bulk of the Ind(PR$_3$)Ni–Me precursor, such that the reaction is fastest with L = PMe$_3$, about 10–20 times slower with L = PPh$_3$ and heterocarbenes, and much slower still with L = PCy$_3$. Comparing the rate constants for these reactions to those of the analogous reactions with PhSiD$_3$ gave the unusually high k_H/k_D ratio of 9.8 ± 0.5 (at 313 K). Taken together, these results suggest that the Si–H activation step likely proceeds through a concerted σ-bond metathesis process. Additional evidence obtained from mechanistic studies of this system point to the involvement of Ind(PR$_3$)Ni–silyl, Ind(PR$_3$)Ni–H, and Ind-free Ni(0) and Ni(II) intermediates in the dehydrogenative oligomerisation of PhSiH$_3$. These assertions have been regrouped to develop the tentative, and somewhat speculative, mechanistic picture illustrated in Scheme 11 [4r].

3.2.3.1.2. Olefin and alkyne polymerisations. The complexes Ind(PR$_3$)Ni–X combine with PMAO to produce noncationic intermediates which can polymerise ethylene into fairly high molecular weight poly(ethylene) (PE) chains at a modest level of activity [4i]. Cationic intermediates are also formed in these reactions and lead to efficient dimerisation of ethylene (vide infra).

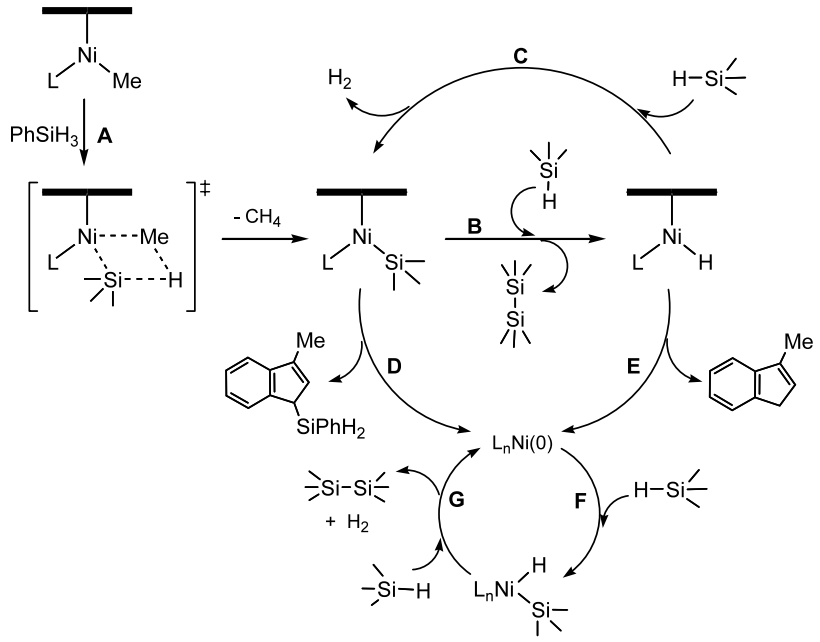

Scheme 11.

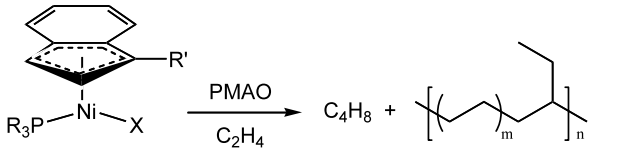

Pre-catalyst			Polymerisation Activity
R	R'	X	Kg of PE (mol of Ni.h)$^{-1}$
Ph	Me	Cl	40
Me	Me	Cl	325
Cy	Me	Cl	310
Ph	i-Pr	Cl	550
Ph	Me	Me	275
Ph	Me	CC-Ph	550

Scheme 12.

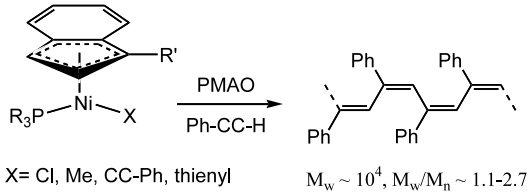

Scheme 13.

Some of the 1-butene thus produced is then incorporated into the growing polymer chain to give PE which is mostly linear but contains a small number of ethyl branches. The best catalytic activities were found in systems having PR_3 = trialkylphosphines, X = Me or CC–Ph, and Ind = 1-*i*-Pr–Ind; the optimal Ni:PMAO ratio seems to be about 1:400 (Scheme 12).

The combination of PMAO and Ind(PR_3)Ni–X can also polymerise Ph–CC–H to *cis*-transoidal poly(phenylacetylene) (PPA) with M_w in the range of $1–6 \times 10^4$ (M_w/M_n ca. 1.3–2.7) (Scheme 13); the analogous reactions with 1-hexyne and 3-hexyne give low M_w oligomers [4g]. The optimal Ni:PMAO ratio in this case seems to be about 1:10; less PMAO significantly reduces the yield of PPA whereas more PMAO leads to smaller M_w polymers. $AlMe_3$ can replace PMAO but the yield of the PPA and its M_w decrease significantly.

These Ni–indenyl complexes represent rare examples of Group 10 metal-based systems for the polymerisation of phenylacetylene. Other Group 10 compounds reported to catalyse alkyne polymerisation include Cp_2Ni, which reacts with Ph–CC–H at 115 °C to give cyclic trimers and PPA with M_w of 460–1600 [39], and a number of Pd and Pt systems that give PPA with M_w in the range of 1000–2000 [40]. In terms of M_w and polydispersity, the PPA obtained from the Ni–indenyl system is comparable to those obtained from most of the reported Rh-based systems [41] with the exception of Noyori's system [42] which promotes a living polymerisation and gives PPA of $M_w \sim 10^6$.

As mentioned above, the Ni–R moiety in these Ind compounds is fairly inert towards insertion with alkynes and alkenes, and so the PMAO is indispensable for the catalysis; however, mechanistic studies of these reactions have failed to determine its precise role in the catalysis.

It is likely that PMAO serves to weaken the Ni–R bond without actually abstracting the Me ligand (i.e. Ni···Me···Al). In this sense, PMAO is more appropriately viewed as a co-catalyst rather than an initiator, because its presence is probably necessary at every insertion step.

3.2.3.1.3. Ligand substitution reactions. All of the catalytic reactions discussed above involve the coordination of one or more substrate molecules to the Ni centre. An important question which arises is whether this step (a) involves the "slippage" of the Ind ligand, (b) requires the pre-dissociation of the PR_3 ligand, or (c) is associative in nature (as is the case for a majority of d^8 systems). These questions have been addressed by a kinetic study of a typical ligand substitution reaction, as described below.

The rate of exchange of PPh_3 in (1-Me–Ind)Ni(PPh_3)Cl by PCy_3 shows a clear dependence on [PCy_3], and the reaction possesses the following activation parameters: $\Delta H^{\ddagger} = 6.40 \pm 0.07$ kcal mol^{-1} and $\Delta S^{\ddagger} = -40 \pm 4$ eu [4k]. Steric factors exert a great influence on the rate of this ligand exchange reaction, as follows. The substitution of PPh_3 by PCy_3 proceeds 100–1000 times more slowly for the more sterically encumbered complex (1-Me–2-Ph–Ind)Ni(PPh_3)Cl (the exchange takes hours to go to completion at room temperature); on the other hand, with the less bulky Cp analogue CpNi(PPh_3)Cl the substitution is essentially over in the time of mixing even at 233 K, i.e. the exchange rate is 10–100 times more rapid for the Cp analogue. These results imply that the phosphine substitution follows an associative mechanism and likely involves the formally 5-coordinate, 18 electron intermediate or activated complex shown in Scheme 14 (assuming an η^3-Ind). This intermediate species is analogous to the proposed intermediates for the polymerisation of Ph–CC–H and ethylene, namely (Ind′)(PR_3)Ni(X)(L) with L being a substrate molecule such as ethylene and X being the growing polymer chain [4k].

It is noteworthy that five coordinate intermediates of the type (π-allyl)NiL_2R have also been postulated in a number of other catalytic reactions [43], while many 5-coordinate d^8 compounds have been shown to be relatively stable species [44]. Although a complex of the type IndNiLL′X (formally 5-coordinate, as in Scheme 14) has not been isolated so far, there is spectroscopic evidence for the existence (in solution) of a closely related analogue wherein the incoming L′ ligand is tethered to the Ind, namely, (η^3,η^1-IndCH_2CH_2-NMe_2)Ni(PPh_3)Cl (Eq. (2)) [4j]:

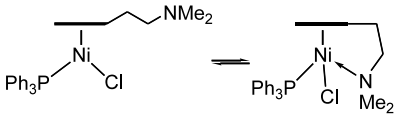

(2)

3.2.3.2. Reactivities of [IndNiL_n]$^+$. As mentioned earlier, abstraction of X^- from IndNiLX or protonation of IndNiLR gives the electronically and coordinatively unsaturated cationic species [Ind(PPh_3)Ni]$^+$. This species can catalyse a number of reactions including the dimerisation of ethylene to butenes, the oligomerisation of styrene, the polymerisation of norbornene, and the co-polymerisation of styrene and norbornene (Scheme 15) [4d,4j]. The catalytic activity is particularly high for the dimerisation of ethylene (ca. 11 000 kg mol of Ni^{-1} h^{-1}) and produces a mixture of mostly butenes; higher oligomers (C_6–C_{20}) can also be produced under different conditions [4d,4i,4q].

The bis(phosphine) complexes [IndNi(PR_3)$_2$]$^+$ are quite inert toward ligand substitution reactions and as such can not be used in catalysis in the absence of co-catalysts. However, a moderate level of catalytic activity can be induced at higher temperatures or in the presence of strong Lewis acids such as PMAO. Thus, norbornene

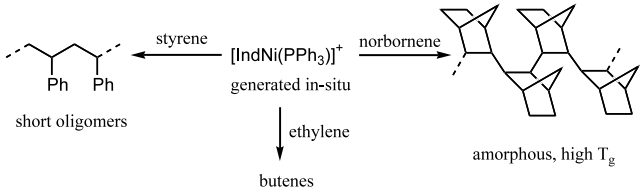

Scheme 15.

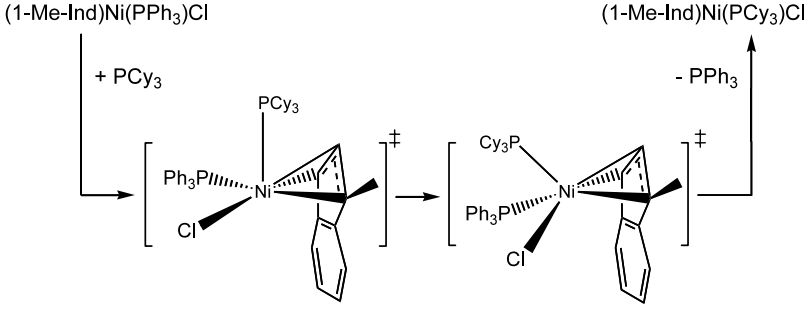

Scheme 14.

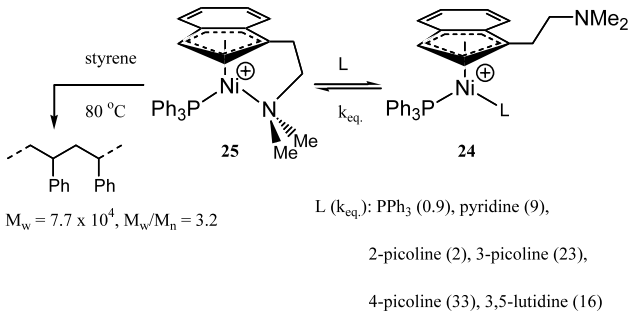

Scheme 16.

can be polymerised (at $<10\%$ yields) in the presence of $[IndNi(PR_3)_2]^+$ at 80 °C or higher [4o]. The complex $[(\eta^3,\eta^1\text{-}1\text{-}CH_2CH_2NMe_2\text{-}Ind)Ni(PPh_3)]^+$ (**25**) is more reactive than the bis(phosphine) derivatives; it initiates the polymerisation of styrene at 80 °C to give a soluble polystyrene ($M_W = 77\,338$ and $M_W/M_N = 3.15$) with turnover numbers of ca. 300–400 [4j]. The analogous reaction with norbornene also requires heating to 80 °C but gives only oligomeric materials ($M_W = 763$; $M_W/M_N = 1.1$) with turnover numbers of 20–40 (Scheme 16).

The above results indicate that the amine tether is displaced more readily than phosphine ligands. Indeed, 1 equiv. of bis(diphenylphosphino)ethane (dppe) displaces both the amine tether and the PPh_3 ligand in **25** to give the complex $[(\eta^3{:}\eta^0\text{-}Ind(CH_2)_2NMe_2)Ni(dppe)][BPh_4]$ (**21**). In contrast, disruption of the N→Ni chelation in **25** by ligands such as PPh_3 or pyridine is much less favourable thermodynamically and requires a large excess of PPh_3 (Scheme 16). These results show that the coordination of the tether in **25** is strong enough to stabilise this compound and prevent the formation of the catalytically inert complex $[(\eta^3{:}\eta^0\text{-}Ind(CH_2)_2NMe_2)Ind)Ni(PPh_3)_2]^+$ (**24a**), yet labile enough to be displaced by relatively strong ligands. Thus, the "hemilabile" character of the amine tether facilitates the use of complex **25** as a single-component precatalyst for the polymerisation of styrene and oligomerisation of norbornene [4j].

Finally, preparation of the complexes $IndNi(PPh_3)OTf$ ($OTf = OSO_2CF_3$) has led to a more convenient route to the cations $[IndNi(PPh_3)L]^+$, and has facilitated the study of the mechanism(s) of olefin oligo- and polymerisations catalysed by the cationic precursors. The key element in these studies is the facile displacement of $[OTf]^-$ by the substrate molecules which are often weak ligands. For instance, the reaction of $(1\text{-}R\text{–}Ind)Ni(PPh_3)OTf$ ($R = {}^i$Pr, Et) with ethylene leads to the dimerisation of ethylene much like the analogous reactions with the in-situ generated cations $[IndNi(PPh_3)]^+$ [4p]. In the reactions between the Ni–OTf precursors and ethylene, the final mixture contained the vinyl-substituted indenes (e.g. $1\text{-}CH_2{=}CH\text{-}3\text{–}{}^i$Pr–IndH); the corresponding reaction with 1-hexene give the 1-hexenyl-substituted indene 1-(1-hexenyl)–3-^{i}Pr–IndH. These results support the mechanistic picture illustrated in Scheme 17.

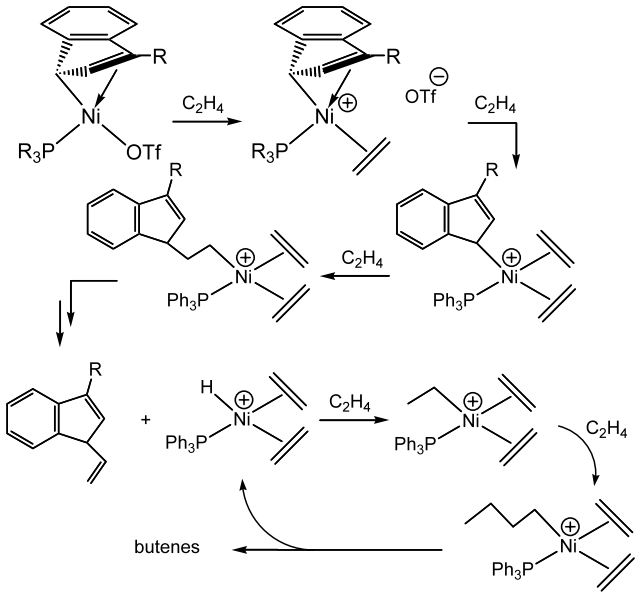

Scheme 17.

4. Concluding remarks

This review has summarised the recent developments in the chemistry of Group 10 metal indenyl complexes. On the structural front, new types of M–Ind interactions have been discovered over the past decade, particularly in the case of Ni complexes, and some progress has been made towards understanding the factors which influence the Ind hapticity. In comparison, most of the analogous Cp complexes display different structural traits [45]. On the reactivity front, some of the elementary reactions of Group 10 metal Ind complexes have been studied and a few catalytic processes have developed, but a great deal more remains to be investigated. It is hoped that future studies will advance our understanding of, for example, the catalytic reactivities of Pd and Pt indenyl complexes. Some of the obvious reactions to elaborate include nucleophilic additions on Ind (in analogy to the well-known Pd–allyl systems), hydrosilylation, carbonylation, etc. In addition, the chemistry of M(IV)–Ind systems should be very interesting, albeit challenging. Overall, these anticipated new advances and the many more unforeseen discoveries which might arise from continued investigations should make the study of Group 10 metal indenyl complexes an interesting area of research.

Acknowledgements

The financial resources put at our disposal by NSERC, FCAR, Université de Montréal, and Québec's Ministère de l'Éducation (Service de la coopération internationale) are gratefully acknowledged. The enthusiastic participation of the members of our group has been pivotal for our studies on the chemistry of Group 10 metal indenyl complexes. Special thanks are due to Frédéric-Georges Fontaine and Laurent F. Groux for reading this review and offering helpful advice.

References

[1] (a) P. Caddy, M. Green, L.E. Smart, N. White, J. Chem. Soc. Chem. Commun. (1978) 839;
(b) A. Borrini, P. Diversi, G. Ingrosso, A. Lucherini, G. Serra, J. Mol. Catal. 30 (1985) 181;
(c) P. Cioni, P. Diversi, G. Ingrosso, A. Lucherini, P. Ronca, J. Mol. Catal. 40 (1987) 337;
(d) T.B. Marder, C.D. Roe, D. Milstein, Organometallics 7 (1988) 1451;
(e) R.S. Tanke, R.H. Crabtree, J. Am. Chem. Soc. 112 (1990) 7984;
(f) H. Brunner, K. Fisch, Angew. Chem. Int. Ed. Engl. 29 (1990) 1131;
(g) A. Ceccon, A. Gambaro, S. Santi, A. Venzo, J. Mol. Catal. 69 (1991) L1;
(h) R.L. Halterman, Chem. Rev. 92 (1992) 965;
(i) B.M. Trost, R.J. Kulawiec, J. Am. Chem. Soc. 114 (1992) 5579;
(j) E. Hauptman, S. Sabo-Etienne, P.S. White, M. Brookhart, J.M. Garner, P.J. Fagan, J.C. Calabrese, J. Am. Chem. Soc. 116 (1994) 8038;
(k) B.Y. Lee, Y.K. Chung, J. Am. Chem. Soc. 116 (1994) 8793.

[2] (a) For a few leading references see: T.M. Frankcom, J.C. Green, A. Nagy, A.K. Kakkar, T.B. Marder, Organometallics 12 (1993) 3688;
(b) M.P. Gamasa, J. Gimeno, C. Gonzalez-Bernardo, B.M. Martìn-Vaca, D. Monti, M. Bassetti, Organometallics 15 (1996) 302.

[3] (a) T. Foo, R.G. Bergman, Organometallics 11 (1992) 1801;
(b) T. Foo, R.G. Bergman, Organometallics 11 (1992) 1811;
(c) P. Caddy, M. Green, J.A.K. Howard, J.M. Squire, N.J. White, J. Chem. Soc. Dalton Trans. (1981) 400.

[4] (a) T.A. Huber, F. Bélanger-Gariépy, D. Zargarian, Organometallics 14 (1995) 4997;
(b) M. Bayrakdarian, M.J. Davis, C. Reber, D. Zargarian, Can. J. Chem. 74 (1996) 2115;
(c) T.A. Huber, M. Bayrakdarian, S. Dion, I. Dubuc, F. Bélanger-Gariépy, D. Zargarian, Organometallics 16 (1997) 5811;
(d) R. Vollmerhaus, F. Bélanger-Gariépy, D. Zargarian, Organometallics 16 (1997) 4762;
(e) F.-G. Fontaine, T. Kadkhodazadeh, D. Zargarian, J. Chem. Soc. Chem. Commun. (1998) 1253;
(f) I. Dubuc, M.-A. Dubois, F. Bélanger-Gariépy, D. Zargarian, Organometallics 18 (1999) 30;
(g) R. Wang, F. Bélanger-Gariépy, D. Zargarian, Organometallics 18 (1999) 5548;
(h) L.F. Groux, F. Bélanger-Gariépy, D. Zargarian, R. Vollmerhaus, Organometallics 19 (2000) 1507;
(i) M.-A. Dubois, R. Wang, D. Zargarian, J. Tian, R. Vollmerhaus, Z. Li, S. Collins, Organometallics 20 (2001) 663;
(j) L.F. Groux, D. Zargarian, Organometallics 20 (2001) 3811;
(k) F.-G. Fontaine, M.-A. Dubois, D. Zargarian, Organometallics 20 (2001) 5156;
(l) T. Kadkhodazadeh, D. Zargarian, unpublished results;
(m) M. Morissette, Sc. Thesis, Université de Montréal, 2002;
(n) L. Groux, D. Zargarian, unpublished results;
(o) F.-G. Fontaine, D. Zargarian, unpublished results;
(p) R. Wang, Ph. D. Thesis, Université de Montréal, 2002;
(q) M.-A. Dubois, M. Sc. Thesis, Université de Montréal, 2000;
(r) F.-G. Fontaine, D. Zargarian, Organometallics 21 (2002) 401;
(s) L.F. Groux, D. Zargarian, Acta Crystallogr. E57 (2001) m547;
(t) R. Wang, L.F. Groux, D.J. Zargarian, J. Organomet. Chem. (2002) in press.

[5] H. Lehmkuhl, J. Näser, G. Mehler, T. Keil, F. Danowski, R. Benn, R. Mynott, G. Schroth, B. Gabor, C. Krüger, P. Betz, Chem. Ber. 124 (1991) 441.

[6] O.N. Babkina, T.A. Bazhenova, N.M. Bravaya, V.V. Streelets, M.Yu. Antipin, K.A. Lysenko, Izv. Akad. Nauk SSSR Ser. Khim. (1996) 1529.

[7] H. Schumann, O. Stenzel, S. Dechert, R.L. Halterman, Organometallics 20 (2001) 1983.

[8] J.R. Ascenso, A.R. Dias, M.T. Duarte, P.T. Gomes, J.N. Marote, A.F.G. Ribeiro, J. Organomet. Chem. 632 (2001) 164.

[9] M.J. Tenorio, M.C. Puerta, I. Salcedo, P. Valerga, J. Chem. Soc. Dalton Trans. (2001) 653.

[10] K. Nakasuji, M. Yamaguchi, I. Murata, K. Tatsumi, A. Nakamura, Organometallics 3 (1984) 1257.

[11] T. Tanase, T. Nomura, T. Fukushima, Y. Yamamoto, K. Kobayashi, Inorg. Chem. 32 (1993) 4578.

[12] (a) J. Vicente, J.-A. Abad, R. Bergs, P.G. Jones, M.C.R. de Arellano, Organometallics 15 (1996) 1422;
(b) J. Vicente, J.-A. Abad, R. Bergs, M.C.R. de Arellano, E. Martinez-Viviente, P.G. Jones, Organometallics 19 (2000) 5597.

[13] (a) F.M. Alias, T.R. Belderrain, M. Paneque, M.L. Poveda, E. Carmona, Organometallics 17 (1998) 5620;
(b) F.M. Alias, T.R. Belderrain, E. Carmona, C. Graiff, M. Paneque, A. Tiripicchio, J. Organomet. Chem. 577 (1999) 316.

[14] D. O'Hare, Organometallics 6 (1987) 1766.

[15] A.J. Hart-Davis, R.J. Mawby, J. Chem. Soc. (A) (1969) 2403.

[16] H.G. Schuster-Woldan, F. Basolo, J. Am. Chem. Soc. 88 (1966) 1657.

[17] A.J. Hart-Davis, C. White, R.J. Mawby, Inorg. Chim. Acta 4 (1970) 441.

[18] D.J. Jones, R.J. Mawby, Inorg. Chim. Acta 6 (1972) 157.

[19] N.N. Turaki, J.M. Huggins, L. Lebioda, Inorg. Chem. 27 (1988) 424.

[20] (a) L.-N. Ji, M.E. Rerek, F. Basolo, Organometallics 3 (1984) 740;
(b) P. Caddy, M. Green, E. O'Brien, L.E. Smart, R. Woodward, Angew. Chem. Int. Ed. Engl. 16 (1977) 648;
(c) P. Caddy, M. Green, E. O'Brien, L.E. Smart, R. Woodward, J. Chem. Soc. Dalton Trans. (1980) 962;
(d) M.E. Rerek, L.-N. Ji, F. Basolo, J. Chem. Soc. Chem. Commun. (1983) 1208;
(e) C.P. Casey, J.M. O'Connor, Organometallics 4 (1985) 384;
(f) H. Bang, T.J. Lynch, F. Basolo, Organometallics 11 (1992) 40.

[21] A number of studies have shown that Ind is a better donor than Cp. For example, electrochemical studies of the complexes (Cp/Ind)Ru(PPh_3)$_2$Cl have shown that the Ru is more easily oxidised while coordinated to Ind (see Ref. 2b), while photoelectron spectroscopy of the complexes (Cp/Ind)RhL_2 (L = ethylene, CO) have shown lower ionisation energies for the nonbonding, metal-based orbitals in the Ind complexes (see Ref. 2a). Similarly, the IR data for the complexes (Cp/Ind)Fe(CO)$_2$R (R = Me and ^{i}Pr) have indicated that the Fe→CO π-backdonation is slightly more pronounced in the Ind series (L. Ambrosi, M. Bassetti, P. Buttiglieri, L. Mannina, D. Monti, G.J. Bocelli, J. Organomet. Chem. 455 (1993) 167). See also Ref. [22].

[22] A.K. Kakkar, N.J. Taylor, N.J. Marder, J.K. Shen, N. Hallinan, F. Basolo, Inorg. Chim. Acta 198–200 (1992) 219.
[23] G.J. Kubas, G. Kiss, C.D. Hoff, Organometallics 10 (1991) 2870.
[24] K.A. Pevear, M.M. Banaszak Holl, G.B. Carpenter, A.L. Rieger, P.H. Rieger, D.A. Sweigart, Organometallics 14 (1995) 512.
[25] H.P. Fritz, F.H. Köhler, K.E. Schwarzhans, J. Organomet. Chem. 19 (1969) 449.
[26] F.H. Köhler, Chem. Ber. 107 (1974) 570.
[27] (a) R.T. Baker, T.H. Tulip, Organometallics 5 (1986) 839;
(b) S.A. Westcott, A.K. Kakkar, G. Stringer, N.J. Taylor, T.B. Marder, J. Organomet. Chem. 394 (1990) 777.
[28] J.S. Merola, R.T. Kacmarcik, D.V. Engen, J. Am. Chem. Soc. 108 (1986) 329.
[29] T.C. Forschner, A.R. Cutler, R.K. Kullnig, Organometallics 6 (1987) 889.
[30] M.J. Calhorda, L.F. Veiros, Coord. Chem. Rev. 185–186 (1999) 37.
[31] P. Seiler, J.D. Dunitz, Acta Crystallogr. B36 (1980) 2255.
[32] R.M. Kowaleski, A.L. Rheingold, W.C. Trogler, F. Basolo, J. Am. Chem. Soc. 108 (1986) 2460.
[33] A.W. Nesmeyanov, N.A. Ustynyuk, L.G. Makarova, V.G. Andrianov, Y.T. Struchkov, S. Andrae, Y.A. Ustynyuk, S.G. Malyugina, J. Organomet. Chem. 159 (1978) 189.
[34] (a) K.R. Gordon, K.D. Warren, Inorg. Chem. 17 (1978) 987;
(b) J.H. Ammeter, J.D. Swalen, J. Chem. Phys. 57 (1972) 678;
(c) L. Pavlik, V. Cerny, E. Maxova, Collect. Czech. Chem. Commun. 35 (1970) 3045.
[35] (a) S. Pasynkiewicz, J. Organomet. Chem. 500 (1995) 283;
(b) N.E. Leadbeater, J. Org. Chem. 66 (2001) 7539.
[36] J.M. Manriquez, M.D. Ward, W.M. Reiff, J.C. Calabrese, N.L. Jones, P.J. Carroll, E.E. Bunel, J.S. Miller, J. Am. Chem. Soc. 117 (1995) 6182.
[37] For a complete review of this subject see: J.Y. Corey, Adv. Silicon Chem. 1 (1991) 327. For a recent report on the dimerisation of silanes by Rh catalysts see: L. Rosenberg, C.W. Davis, J.J. Yao, J. Am. Chem. Soc. 123 (2001) 5120.
[38] (a) F. Gauvin, J.F. Harrod, H.-G. Woo, Adv. Organomet. Chem. 42 (1998) 363;
(b) Y. Obora, M. Tanaka, J. Organomet. Chem. 595 (2000) 1.
[39] W.E. Douglas, A.S. Overend, J. Organomet. Chem. 444 (1993) C62 (and references cited therein).
[40] A. Furlani, S. Licoccia, M.V. Russo, A. Camus, N. Marsich, J. Polym. Sci.: Part A: Polym. Chem. 24 (1986) 991.
[41] (a) A. Furlani, C. Napoletano, M.V. Russo, W.J. Feast, Polym. Bull. 16 (1986) 311;
(b) Y. Goldberg, H. Alper, J. Chem. Soc. Chem. Commun. (1994) 1209.
[42] (a) Y. Kishimoto, P. Eckerle, T. Miyatake, T. Ikariya, R. Noyori, J. Am. Chem. Soc. 116 (1994) 12131;
(b) Y. Kishimoto, T. Miyatake, T. Ikariya, R. Noyori, Macromolecules 29 (1996) 5054.
[43] (a) B. Bosnich, P.B. Mackenzie, Pure Appl. Chem. 54 (1982) 189;
(b) M. Cherest, H. Felkin, J.D. Umpleby, S.G. Davies, J. Chem. Soc. Chem. Commun. (1981) 681;
(c) G. Consiglio, O. Piccollo, L. Roncetti, F. Morandini, Tetrahedron 42 (1986) 2043;
(d) H. Kurosawa, J. Organomet. Chem. 334 (1987) 243.
[44] (a) For a few trigonal bipyramidal compounds of d^8 metals with tripodal tetradentate ligands see: S.-i. Aizawa, T. Ilida, S. Funahashi, Inorg. Chem. 35 (1996) 5163 (and references cited therein);
(b) For a few 5-coordinate complexes of Rh(I) with multidentate imine ligands see: H.F. Haarman, F.R. Bregman, J.-M. Ernsting, N. Veldman, A.L. Spek, K. Vrieze, Organometallics 16 (1997) 54 (and references cited therein);
(c) For square pyramidal Pd(II) complexes of the type $(PR_3)_3PdX_2$ see: W.J. Louw, D.J.A. de Waal, G.J. Kruger, J. Chem. Soc. Dalton Trans. (1976) 2364 and J.W. Collins, F.G. Mann, D.G. Watson, H.R. Watson, J. Chem. Soc. (1964) 1803;
(d) For a trigonal bipyramidal ethylene complex of Pt(II) see: L. Maresca, G. Natile, M. Calligaris, P. Delise, L. Randaccio, J. Chem. Soc. Dalton Trans. (1976) 2386.
[45] For a detailed analysis of Ni–Cp interactions see: P. Holland, M.E. Smith, R.A. Andersen, R.G. Bergman, J. Am. Chem. Soc. 119 (1997) 12815.
[46] A.K. Kakkar, G. Stringer, N.J. Taylor, T.B. Marder, Can. J. Chem. 73 (1995) 981.
[47] T. Foo, R.G. Bergman, Organometallics 11 (1992) 1801.
[48] T.L. Husebo, C.M. Jensen, Organometallics 14 (1995) 1987.
[49] M. Mlekuz, P. Bougeard, B.G. Sayer, M.J. McGlinchey, C.A. Rodger, M.R. Churchill, J.W. Ziller, S.-K. Kang, T.A. Albright, Organometallics 5 (1986) 1656.
[50] A.K. Kakkar, N.J. Taylor, J.C. Calabrese, W.A. Nugent, D.C. Roe, E.A. Connaway, T.B. Marder, J. Chem. Soc. Chem. Commun. (1989) 990.
[51] T.B. Marder, J.C. Calabrese, D.C. Roe, T.H. Tulip, Organometallics 6 (1987) 2012.